1521-0111/92/1/88–99$25.00
MOLECULAR PHARMACOLOGY

https://doi.org/10.1124/mol.117.108563
Mol Pharmacol 92:88–99, July 2017

Rapid Throughput Analysis of $GABA_A$ Receptor Subtype Modulators and Blockers Using DiSBAC$_1$(3) Membrane Potential Red Dye[S]

Atefeh Mousavi Nik, Brandon Pressly, Vikrant Singh, Shane Antrobus, Susan Hulsizer, Michael A. Rogawski, Heike Wulff, and Isaac N. Pessah

Department of Molecular Biosciences, School of Veterinary Medicine (A.M.N., S.A., S.H., I.N.P.), and Department of Pharmacology (B.P., V.S., M.A.R., H.W.), School of Medicine, University of California Davis, Davis, California; Department of Neurology, School of Medicine, University of California Davis, Sacramento, California (M.A.R.); and The Medical Investigation of Neurodevelopmental Disorders Institute, Sacramento, California (I.N.P.)

Received February 10, 2017; accepted April 12, 2017

ABSTRACT

Fluorometric imaging plate reader membrane potential dye (FMP-Red-Dye) is a proprietary tool for basic discovery and high-throughput drug screening for G-protein-coupled receptors and ion channels. We optimized and validated this potentiometric probe to assay functional modulators of heterologous expressed $GABA_A$ receptor ($GABA_AR$) isoforms (synaptic $\alpha1\beta3\gamma2$, extrasynaptic $\alpha4\beta3\delta$, and $\beta3$ homopentomers). High-resolution mass spectrometry identified FMP-Red-Dye as 5,5′-(1-propen-1-yl-3-ylidene)bis[1,3-dimethyl-2-thio-barbituric acid]. $GABA_AR$-expressing cells equilibrated with FMP-Red-Dye exhibited depolarized equilibrium membrane potentials compared with $GABA_AR$-null cells. The channel blockers picrotoxin, fipronil, and tetramethylenedisulfotetramine, and the competitive antagonist bicuculline reduced fluorescence near the levels in $GABA_AR$-null cells indicating that FMR-Red-Dye, a barbiturate derivative, activates $GABA_AR$-mediated outward Cl^- current in the absence of GABA. GABA caused concentration-dependent increases in fluorescence with rank order of potencies among $GABA_AR$ isoforms consistent with results from voltage-clamp experiments (EC_{50} values for $\alpha4\beta3\delta$, $\alpha1\beta3\gamma2$, and β_3 homopentamers were 6 ± 1, 40 ± 11, and >18 mM, respectively), whereas $GABA_AR$-null cells were unresponsive. Neuroactive steroids (NAS) increased fluorescence of $GABA_AR$ expressing cells in the absence of GABA and demonstrated positive allosteric modulation in the presence of GABA, whereas benzodiazepines only exhibited positive allosteric modulator (PAM) activity. Of 20 NAS tested, allopregnanolone, (3α,5α,20E)-3-hydroxy-13,24-cyclo-18-norcholan-20-ene-21-carbonitrile, eltanolone, 5β-pregnan-3α,21-diol-20-one, and ganaxolone showed the highest potency. The FMP-Red-Dye–based assay described here provides a sensitive and quantitative method of assessing the activity of $GABA_AR$ agonists, antagonists, and PAMs on diverse $GABA_AR$ isoforms. The assay has a wide range of applications, including screening for antiseizure agents and identifying channel blockers of interest to insecticide discovery or biosecurity.

Introduction

$GABA_A$ receptors ($GABA_ARs$) are ligand-gated anion channels that mediate inhibition in the mammalian central nervous system by responding to the neurotransmitter GABA (Barnard et al., 1998).$GABA_AR$ dysfunctions are associated with epilepsy, autism, fragile X syndrome, depression, and schizophrenia (Verkman and Galietta, 2009; Stafstrom et al., 2012; Rudolph and Möhler, 2014; Braat and Kooy, 2015). $GABA_ARs$ are also the primary toxicological targets of several currently used insecticides (e.g., fipronil) and pesticides of historical importance that persist in the environment (e.g., organochlorines) (Casida and Durkin, 2015). Importantly, $GABA_ARs$ are a major pharmacological target for antiseizure drugs (Brodie et al., 2016).

$GABA_ARs$ are pentameric anion channels composed of two α subunits, two β subunits, and one subunit that is designated as γ, δ, ε, θ, or π. There are multiple isoforms of many of the subunits (six for α, three for β, and three for γ), allowing for a high degree of variation depending on brain region and developmental stage. Most synaptic $GABA_ARs$ contain two α subunits, two β subunits, and one $\gamma2$ subunit; have a relatively

This work was sponsored by the National Institutes of Health National Institute of Neurologic Disorders and Stoke [UC Davis CounterACT Center of Excellence Grant U54 NS 011269] and Intellectual and Developmental Disabilities Research Center (IDDRC) Core Center [Grant U54 HD079125]; B.P. was supported by a National Institutes of Health National Institute of General Medical Sciences funded Pharmacology Training Program [Grant T32GM099608].
https://doi.org/10.1124/mol.117.108563.
[S] This article has supplemental material available at molpharm.aspetjournals.org.

ABBREVIATIONS: DiSBAC$_1$(3), 5,5′-(1-propen-1-yl-3-ylidene)bis[1,3-dimethyl-2-thio-barbituric acid]; E_m, equilibrium membrane; FLIPR, fluorometric imaging plate reader; FMP-Red-Dye, fluorometric imaging plate reader membrane potential red dye; $GABA_AR$, $GABA_A$ receptor; HEK, human embryonic kidney; NAS, neuroactive steroids; PAM, positive allosteric modulator; PTX, picrotoxin; TBPS, *t*-butylbicyclophosphorothionate; TETS, tetramethylenedisulfotetramine; 5β,3α-THDOC, 3α,21-dihydroxy-5β-preganan-20-one; XJ-42, (3α,5α,20E)-3-hydroxy-13,24-cyclo-18-norcholan-20-ene-21-carbonitrile.

low affinity for GABA; and mediate fast phasic inhibition (Rissman and Mobley, 2011; Brickley and Mody, 2012). In contrast, extrasynaptic $GABA_ARs$ often contain a δ subunit, have a higher affinity for GABA, and mediate persistent tonic inhibition (Bettler and Tiao, 2006; Belelli et al., 2009; Brickley and Mody, 2012). In addition to the endogenous neurotransmitter, GABA, which binds to the interface of α and β subunits, $GABA_ARs$ possess binding sites for neuroactive steroids (NAS), benzodiazepines, and barbiturates that allosterically enhance GABA-activated Cl^- conductance and in some instances activate Cl^- conductance in the absence of GABA, thereby exerting anxiolytic, sedative, and antiseizure effects that are useful for treating anxiety and sleep disorders and epilepsy, as well as serving as general anesthetics (Belelli and Lambert, 2005; Herd et al., 2007). The benzodiazepine binding site is localized between the α and γ subunits, whereas NAS are known to have two binding sites, a potentiation site on the α subunit and a direct activator site in the α/β interface, both of which need to be occupied for potent channel activation (Akabas, 2004;Campagna-Slater and Weaver, 2007; Hosie et al., 2007; Alvarez and Estrin, 2015). Although the precise sites to which barbiturates bind remain elusive, domains within β subunit transmembrane segments TM2 and TM3 appear to be critical (Löscher and Rogawski, 2012). Interestingly, $\beta 3$ subunits reconstitute a homopentameric channel that possesses NAS binding sites (Chen et al., 2012; Miller and Aricescu, 2014; Alvarez and Estrin, 2015).

Considering the utility of $GABA_ARs$ as therapeutic targets, there is substantial interest in the identification of improved $GABA_AR$ modulators. A suitable high-throughput screening method would significantly aid in the identification of such agents. One potential method to assess $GABA_AR$ function in a high-throughput manner uses the fluorometric imaging plate reader (FLIPR) membrane potential red dye (FMP-Red-Dye) that redistributes across the plasma membrane in a voltage-dependent manner. Cell depolarization results in dye movement into the cell and binding to intracellular proteins and hydrophobic sites causing increased florescence signals and vice versa for hyperpolarization. Thus, FMP-Red-Dye allows monitoring of membrane potential changes in a bidirectional fashion independent of ion type. FMP-Red-Dye is convenient in that it does not require cells to be washed of excess dye after equilibration due to inclusion of a proprietary cell membrane impermeant red wavelength quencher, which results in a high signal-to-noise ratio (Fairless et al., 2013). Mennerick et al. (2010) reported that many voltage-sensitive dyes such as Di-4-ANEPPS and $DiBAC_4(3)$ can directly activate and/or potentiate $GABA_AR$ currents in a manner similar to NAS and barbiturates, questioning their usefulness for screening $GABA_AR$ ligands. A previous study reported that FMP-Red-Dye had better performance than FMP-Blue-Dye, and that it produced results comparable to electrophysiology (Joesch et al., 2008). However, the chemical identity of FMP-Red-Dye is proprietary and the degree to which its constituents might influence $GABA_AR$ function, and therefore limit the dye's usefulness in characterizing $GABA_AR$ modulators, has remained unclear.

Here, we identify the voltage-sensitive component of FMP-Red-Dye as 5,5′-(1-propen-1-yl-3-ylidene)bis[1,3-dimethyl-2-thio-barbituric acid] [$DiSBAC_1(3)$]; optimize and validate its use as a rapid throughput indicator of $GABA_AR$ activators, blockers, and positive allosteric modulators (PAMs) using FLIPR; and implement the assay to screen a small library of NAS and channel blockers. We show that FMP-Red-Dye can be used to differentiate $GABA_AR$-mediated responses in cell lines that stably or transiently express synaptic ($\alpha 1\beta 3\gamma 2$), extrasynaptic ($\alpha 4\beta 3\delta$), or $\beta 3$ homomeric $GABA_AR$ isoforms. We conclude that the FMP-Red-Dye–based assays provide sensitive and quantitative approaches to investigate functional drug effects on $GABA_AR$ isoforms, whether they are mediated by binding to the GABA recognition site, the NAS PAM sites, or convulsant channel blocking sites. The assay is useful for antiseizure drug screening and identifying novel channel blockers of interest to insecticide discovery or biosecurity.

Materials and Methods

Reagents

Poly-L-lysine, cytosine arabinoside, picrotoxin (PTX), *t*-butylbicyclophosphorothionate (TBPS), fipronil, bicuculline, diazepam, and GABA were purchased from Sigma Aldrich (St. Louis, MO). Falcon 96-Well Imaging Plates with lids were purchased from Fisher Scientific (Hampton, NH). FLIPR Membrane Potential Red Assay Kit (FMP-Red-Dye) was purchased from Molecular Devices Corporation (Sunnyvale, CA). Fluo4-AM was purchased from Life Technology (Hampton, NH). GS21 supplement was purchased from MTI-Global Stem (Gaithersburg, MD). Org 20599, alphaxalone, eltanolone, progesterone, and midazolam were purchased from Tocris (Pittsburgh, PA). (3α,5α,20E)-3-Hydroxy-13,24-cyclo-18-norcholan-20-ene-21-carbonitrile (XJ-42) (compound 63 in Covey and Jiang, 2014) was a generous gift of Dr. Douglas F. Covey (Washington University School of Medicine, St. Louis, MO), 3-[3α-hydroxy-3β-methyl-5α-androstan-17β-yl]-5-(hydroxymethyl)isoxazole (Hogenkamp et al., 2014) was a generous gift of Dr. Kelvin W. Gee (University of California, Irvine, Irvine CA). Allopregnanolone was custom synthesized by SAFC Pharma (Madison, WI). Dehydroepiandrosterone sulfate, indiplon, and ursodeoxycholic acid (sodium salt) were purchased from Cayman Chemical (Ann Arbor, MI). Dehydroepiandrosterone acetate, dehydroepiandrosterone, cortisol, epiandrosterone, 20α-dihydropregnenolone, androstenediol, etiocholanolone, androsterone, alphadolone 21-acetate, and tetrahydrocortexone were purchased from Steraloids (Newport, RI). Tetramethylenedisulfotetramine (TETS) was synthesized in the laboratory of Dr. Bruce Hammock as previously described (Zhao et al., 2014). All reagents were >97% purity.

Heterologous Expression of $GABA_AR$ Isoforms

Expression of $GABA_AR$ Subunits for Potentiometric Measurements with FLIPR FMP-Red-Dye. Our goal was to develop a reliable, rapid throughput approach to quantitatively assess the influences of blockers, antagonists, and PAMs on the functional activity of diverse $GABA_AR$ isoforms. To this end, we investigated cell lines that stably or transiently express three $GABA_AR$ isoforms of different subunit compositions. A human embryonic kidney (HEK) 293 cell line that stably expresses human $GABA_AR$ $\alpha 1\beta 3\gamma 2$ subunits (CYL3053 PrecisION hGABA-A $\alpha 1/\beta 3/\gamma 2$-HEK Recombinant Cell Line) was a generous gift of EMD Millipore Corporation, St. Charles, MO. $GABA_AR$ $\alpha 1\beta 3\gamma 2$ heteropentomeric channels primarily localize to synaptic sites in mammalian neurons (McCartney et al., 2007). The $GABA_AR$-null HEK 293 line, which served as the control, was purchased from American Type Culture Collection (ATCC-CRL-1573) (Manassas, VA). Upon arrival both cell lines were expanded in Dulbecco's modified Eagle's medium/Ham's F-12 (50/50 mix), 10% fetal bovine serum, 1% nonessential amino acid (Invitrogen, Carlsbad, CA) at 37°C in 5% CO_2 and several bullets were frozen to limit passage numbers. Cells expressing $\alpha 1\beta 3\gamma 2$ subunits were kept under selection pressure with 400 μg/ml genticin, 100 μg/ml hygromycin B (Invitrogen), and

0.625 μg/ml puromycin (Clontech, Mountain View, CA). $GABA_AR$-null cells were cultured in 100 U/ml penicillin and 100 μg/ml streptomycin (Gibco, Waltham, MA) to minimize the risk of bacterial contamination. Cell lines were discarded after 15 passages. Cells were passaged when 70%–80% confluent and harvested using 0.05% trypsin-EDTA and 50,000–60,000 cells/well (in a volume of 100 μl), seeded into poly-L-lysine–coated wells of a 96-well plate, and allowed to recover in the incubator overnight before FMP-Red-Dye loading and measurements of equilibrium membrane (E_m) potential with FLIPR.

A L-tk (mouse connective tissue) cell line expressing the human $GABA_AR$ $\alpha4\beta3\delta$ subunit combination under a dexamethasone-inducible promoter was kindly provided by Dr. Trevor Smart (University College, London) (Brown et al., 2002). The $\alpha4\beta3\delta$ subunit isoform is found at extrasynaptic sites in mammalian brain. The L-tk cell line was cultured in Dulbecco's modified Eagle's medium plus glutamine, 4.5 g/l Na pyruvate, and glucose with 10% fetal bovine serum, in the presence of 1 mg/ml genticin and 0.2 mg/ml zeocin to select $\alpha4\beta3\delta$-positive cells. Dexamethasone (1 μM; Invitrogen) or vehicle was added to the media to induce $\alpha4\beta3\delta$ subunit expression or serve as $GABA_AR$-null cells, respectively, when 80%–90% confluent. Cells were induced for 48 hours, passaged using trypsin-EDTA 0.05%, plated at 50,000–60,000 cells/well into 96-well plates, and after 24-hour recovery loaded with FMP-Red-Dye and membrane potential measured as described subsequently.

Transient expression of $GABA_AR$ $\beta3$ homopentamers in HEK 293 cells (ATCC CRL-1573) was achieved with a pcDNA3.1 expression vector generously provided by Dr. Robert L. Macdonald (Vanderbilt University, Nashville, TN). HEK 293 cells were cultured as described previously. Twenty-four hours before transfection, cells were plated on 10-cm tissue culture–treated dishes and transfected with plasmid DNA at 70%–90% confluence using TurboFect (Thermo Scientific, Waltham, MA) according to the manufacturer's instructions. At 24-hour post-transfection, cells were dissociated with trypsin, counted, and plated on poly-L-lysine–coated 96-well plates (Falcon, Waltham, MA) at a density of 50,000–60,000 cells/well. All FLIPR experiments were carried out 48 hours post-transfection.

Expression of $GABA_AR$ Subunits for Electrophysiological Measurements. The human $GABA_AR$ $\alpha1$, $\beta3$, and $\gamma2$ cloned into pcDNA3.1 expression vectors were a gift from Dr. Robert L. Macdonald (Vanderbilt University). Fibroblast L929 cells were cultured in Dulbecco's modified Eagle's medium (Lonza, Portsmouth, NH) supplemented with 10% fetal bovine serum, 100 U/ml penicillin, and 100 mg/ml streptomycin (Invitrogen) and maintained in humidified 95% air and 5% CO_2 air at 37°C. Cells were transfected using FuGENE 6 (Roche, Santa Clara, CA) transfection reagent with an equal amount of each of the subunits in combination with pEGFP-C1. The transfection ratio of total cDNA to transfection reagent was 2:1 with equal amounts of $\alpha1$, $\beta3$, and $\gamma2$ cDNA to reconstitute synaptic $\alpha1\beta3\gamma2$ $GABA_AR$, or $\beta3$ alone to reconstitute homopentamers. Two days post-transfection, cells were plated on glass coverslips and transfected cells were identified using an epifluorescence microscope for electrophysiological measurements. Electrophysiological recordings from L-tk cells expressing $GABA_AR$ $\alpha4\beta3\delta$ subunit composition were obtained with culture and induction methods described previously.

Rapid Throughput Analysis of $GABA_AR$ Modulators Using FLIPR FMP-Red-Dye

Once HEK 293 and L-tk cells were cultured on 96-well plates for 24 hours, FMP-Red-Dye was reconstituted to 1× with 100 ml of Locke's buffer (NaCl 154 mM, KCl 5.6 mM, $CaCl_2$ 2.3 mM, $MgCl_2$ 1 mM, HEPES 8.6 mM, glucose 5.6 mM, glycine 0.1 μM, pH 7.4) as recommended by the supplier (Molecular Devices Corporation). Growth medium was removed from the wells and cells were loaded with 100 μl FMP-Red-Dye solution for 30 minutes in the dark at room temperature (except for the experiments in Fig. 1 where fluorescence signals were recorded immediately). Each plate was transferred to the FLIPR Tetra Station; the dye was excited at 510–545 nm, and the fluorescent signals were recorded at 565–625 nm. Baseline recordings were acquired for 2 minutes at a sampling rate of 1 Hz (400 ms of illumination per sample). FMP-Red-Dye is a slow-response, potential-sensitive probe and the maximal response is usually seen within

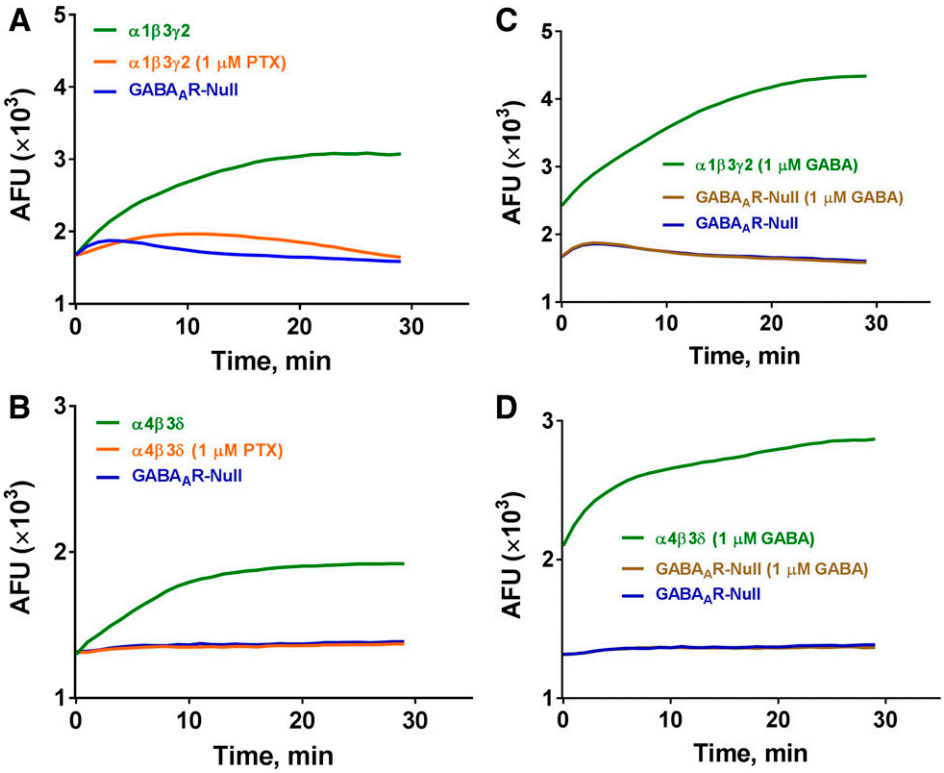

Fig. 1. FMP-Red-Dye modulates $\alpha1\beta3\gamma2$ and $\alpha4\beta3\delta$ $GABA_ARs$ expressed in HEK 293 and L-tk cells, respectively. (A and B) FMP-Red-Dye causes a slow increase in fluorescence [arbitrary florescence units (AFUs)] in cells expressing both receptor types over a 30-minute period that is blocked by 1 μM PTX. The AFU value in $GABA_AR$-null cells minimally changes during the 30 minutes after onset of FMP-Red-Dye exposure. (C and D) GABA (1 μM) causes an instantaneous increase in AFUs in cells expressing both receptors types compared with $GABA_AR$-null cells; the AFU continues to slowly rise over 30 minute. GABA has no effect on AFUs in $GABA_AR$-null cells.

2 minutes after triggering cellular depolarization or hyperpolarization (see Figs. 3 and 4) (Dasheiff, 1985). Cell responses were normalized by calculation $(F_{max} - F_{min})/F_{min} = \Delta F/F_0$, where F_{max} was the maximum response in arbitrary fluorescence units, and F_{min} was the baseline arbitrary florescence unit value. Although HEK 293 cells were unresponsive to vehicle additions, signals from L-tk cells expressing $\alpha_4\beta_3\delta$ subunits exhibited an abrupt but transient drop in fluorescence with addition of any solution, including Locke's or vehicle, and therefore all data from L-tk cells were normalized to vehicle baseline by subtraction.

Electrophysiological Recordings

Whole-cell voltage-clamp and current-clamp recordings were performed at room temperature with an EPC-10 amplifier (HEKA, Holliston, MA). Cells were bathed in an external Ringer's solution consisting of 160 mM NaCl, 4.5 mM KCl, 1 mM $MgCl_2$, 2 mM $CaCl_2$, and 10 mM HEPES with pH 7.4 and 311 mOsm. Recording electrodes were pulled and fire-polished to resistances of 1.8–2.4 MΩ for voltage-clamp and 3–6 MΩ for current-clamp experiments. Electrodes were filled with an internal solution consisting of 154 mM KCl, 2 mM $CaCl_2$, 1 mM $MgCl_2$, 10 mM HEPES, and 10 mM EGTA with pH 7.3 and 308 mOsm. Cells were voltage clamped at −80 mV and control currents were recorded under the application of 1 μM GABA, using a gravity-fed fast perfusion system, for 5 seconds followed by a 40–50 second wash with external solution. GABA concentration-response relationships were determined by testing increasing concentrations of GABA and normalizing GABA currents to the peak response induced by a saturating concentration of GABA. Normalized currents were fitted using the Hill equation (n_H) to determine the EC_{50} and EC_{10} values. The EC_{10} value (1 μM) was used to evaluate the positive modulatory effects of the neurosteroids. The increases in Cl^- current elicited in the presence of NAS were compared with the initial EC_{10} value to determine the fold increase in current. Test solutions of the NAS were freshly prepared immediately before each application onto cells. Membrane potential was recorded on the initial break into the cell while in current-clamp mode. For experiments involving FMP-Red-Dye, cells were preincubation with the dye for 30 minutes before recording in the absence or presence of fipronil. Cells were then exposed to 10 minutes of UV irradiation (460–490 nm) to induce the previously reported photodynamic effect of voltage-sensitive dyes (Mennerick et al., 2010).

Data Analysis

GraphPad Prism software (version 6; GraphPad Software, La Jolla, CA) was used for statistical analysis and graphing. The EC_{50} values were determined using nonlinear regression with a four-parameter logistic equation. Student's t test or F test ($P < 0.05$) was applied to determine statistical differences. For post hoc multiple comparisons separate one-way analysis of variance (for EC_{50} and slope) using Tukey's test was applied. Data are presented as the mean ± S.D. as stated. For electrophysiology, data analysis was performed using Excel (Microsoft) and Origin 7.0 (OriginLab Corp., Northhampton, MA) software. Data fitting to the Hill equation to obtain the EC_{50} values was performed with Origin 7.0. Data are presented as the mean ± S.D.

Results

Optimization and Evaluation of FMP-Red-Dye Assay for Functional $GABA_AR$ Screening. In the initial experiments, HEK 293 cells stably expressing one of the widely expressed human synaptic $GABA_AR$ isoforms $\alpha1\beta3\gamma2$ or $GABA_AR$-null HEK 293 cells were used to test whether FMP-Red-Dye potentiates $GABA_AR$ function in the absence of GABA as reported for other potentiometric dyes (Mennerick et al., 2010). FMP-Red-Dye signals were monitored in real-time within 1 minute after dye addition to the cell medium. Initial fluorescence signals were similar for both $GABA_AR$-expressing and $GABA_AR$-null HEK 293 cells, but equilibrated to different steady-state fluorescence signals within 30 minutes, with $\alpha1\beta3\gamma2$-expressing HEK 293 cells invariably achieving 2-fold higher steady-state fluorescence intensity than the respective null cells (Fig. 1A). Importantly, inclusion of PTX (1 μM) with dye addition prevented the rise in fluorescence in $GABA_AR$-expressing cells (Fig. 1A). In contrast, inclusion of GABA (1 μM) with the potentiometric dye caused an instantaneous increase in dye signal (within the 1 Hz resolution of the recording) followed by a more gradual equilibration of fluorescence to a 3-fold greater signal than that achieved in null cells by 30 minutes (Fig. 1C). $GABA_AR$-null cells showed a minimal time-dependent fluctuation in fluorescence and this response was unchanged by the presence of GABA. Similar results were obtained in studies comparing FMP-Red-Dye responses in L-tk cells expressing the extrasynaptic $\alpha4\beta3\delta$ $GABA_AR$ isoform with L-tk $GABA_AR$-null cells (Fig. 1, B and D). These results indicate that by itself FMP-Red-Dye promotes slow depolarization of cells expressing either synaptic or extrasynaptic $GABA_AR$ subunits but fails to cause this effect in the respective null cells. FMP-Red-Dye–induced cell depolarization was prevented by PTX, indicating that it requires functional $GABA_ARs$. In contrast to the apparent slow activation of $GABA_AR$ caused by FMP-Red-Dye, GABA induced a rapid activation of the receptors.

To further verify the accuracy of our interpretation, FMP-Red-Dye was equilibrated for 30 minutes with $\alpha1\beta3\gamma2$-expressing or $GABA_AR$-null HEK 293 cells and membrane potential recorded in the current-clamp mode of the patch-clamp technique. While null HEK cells had a resting membrane potential of −78.6 ± 6.3 mV, which did not significantly change after incubation with FMP-Red-Dye (Fig. 2), $\alpha1\beta3\gamma2$-expressing HEK 293 cells had a more positive resting membrane potential of −68.8 ± 6.6 mV ($P = 0.02$), which was depolarized by a further 9 mV to −59.6 ± 6.9 mV ($P = 0.03$) after incubation with FMP-Red-Dye for 30 minutes. This depolarization could be prevented by the $GABA_AR$ blocker fipronil (Fig. 2). Interestingly, 10 minutes of UV irradiation (460–490 nm) induced the previously reported photodynamic effect of voltage-sensitive dyes (Mennerick et al., 2010), and induced a further depolarization of the $\alpha1\beta3\gamma2$-expressing HEK cells to −42.8 ± 10.1 mV ($P = 0.002$) (Fig. 2).

The light-dependent influences of FMP-Red-Dye on cells expressing $GABA_AR$ isoforms compelled us to determine its chemical identity, which to date has been proprietary information. The excitation and emission characteristics of the red dye (excitation 470/emission 580 nm) suggest that the dye is a member of one of two structurally related families of voltage-sensitive dyes, DiBAC and/or DiSBAC. These dyes, which are derivatives of barbituric or thiobarbituric acid (Supplemental Fig. 1A), may bind at the barbiturate binding sites of the $GABA_AR$ (Mennerick et al., 2010). High-resolution mass spectrometry was used to elucidate the molecular identity of FMP-Red-Dye in its complex matrix. An experimental molecular mass of 379.0521 was obtained (Supplemental Fig. 1B), which is within 5 ppm of the theoretical molecular mass of 379.0534 of the voltage-sensitive dye 5,5′-(1-propen-1-yl-3-ylidene)bis[1,3-dimethyl-2-thio-barbituric acid [$DiSBAC_1(3)$; CID 53485318].

Collectively, these results suggested that under tightly controlled experimental conditions the FMP-Red-Dye FLIPR

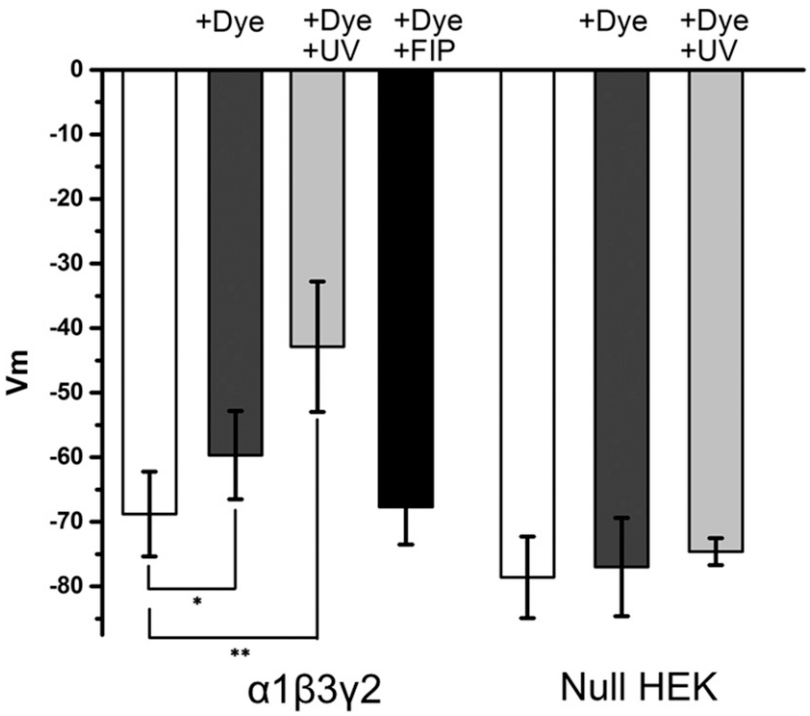

Fig. 2. Current clamp experiments demonstrating that incubation with FMP-Red-Dye leads to a depolarization of $GABA_AR$-expressing cells. Membrane potential (V_m) values of $\alpha1\beta3\gamma2$ expressing HEK 293 cells and $GABA_AR$-null HEK 293 cells measured by current clamp under three conditions: 1) no treatment; 2) incubation with FMP-Red-Dye for 30 minutes prior to recording membrane potential in the absence or presence of 50 μM fipronil (FIP); and 3) incubation with FMP-Red-Dye for 30 minutes followed by 10 minutes of UV irradiation prior to recording membrane potential; n = 8–10 cells per condition. Unpaired t test was used to compare the treatments with control (white bar). $^*P < 0.05$, $^{**}P < 0.01$. Each bar represents mean ± S.D.

platform could provide a sensitive and quantitative method for investigating pharmacological responses of $GABA_AR$ isoforms to diverse direct $GABA_AR$ activators, $GABA_AR$ channel blockers of toxicological significance, and $GABA_AR$ PAMs. To these ends, subsequent experiments were conducted following 30 minutes equilibration of cells seeded in 96-well plates with dye in the dark, followed by 2 minutes of baseline recording and 10 minutes of response recording after drug addition from a 96-well source plate. Excitation and emission were within visible wavelengths (excitation 510–545 nm/emission 565–625 nm), and wells were excited by 400 ms duration pulsed illumination at a rate of 1 Hz. This protocol minimizes photodynamic influences of the FMP-Red-Dye, which may alter its activity on $GABA_ARs$.

Differential Potencies of GABA toward Activating Synaptic and Extrasynaptic $GABA_AR$. Concentration-response relationships for GABA were obtained using the FMP-Red-Dye assay in heterologous cells expressing either the synaptic $GABA_AR$ isoform $\alpha1\beta3\gamma2$ or the extrasynaptic isoform $\alpha4\beta3\delta$. Figure 3A shows representative responses to a range of GABA concentrations from 0.1 nM to 30 μM. The respective $GABA_AR$-null HEK 293 or L-tk cells, in contrast, did not respond to GABA. The concentration-response curves in Fig. 3B (left) indicate that GABA was significantly more potent at eliciting a fluorescence signal in cells expressing $\alpha4\beta3\delta$ than in cells expressing $\alpha1\beta3\gamma2$ (EC_{50} values, 6 ± 1 nM, 95% confidence interval: 4–16 and 40 ± 11 nM; 95% confidence interval: 30–53 nM, respectively). HEK 293 cells expressing homopentameric $\beta3$ subunits were largely insensitive to GABA at concentrations ≤ 1 mM, although these cells did exhibit fluorescence responses to higher concentrations of GABA that were sensitive to PTX (see Fig. 5).

Voltage-clamp experiments performed with cells expressing the same subunit compositions used in the FMP-Red-Dye experiments confirmed that the cells expressing $\alpha4\beta3\delta$ $GABA_AR$ were more sensitive to GABA than those expressing $\alpha1\beta3\gamma2$ subunits ($P < 0.05$) (Fig. 3B, right). Comparing results using the two approaches indicated that the FMP-Red-Dye assay was a very sensitive measurement of GABA-triggered depolarization. Regardless, with both experimental approaches $\alpha4\beta3\delta$ was more sensitive to GABA than $\alpha1\beta3\gamma2$ (7-fold for FMP-Red-Dye assay and 12-fold for the patch-clamp technique).

Whether FMP-Red-Dye itself was directly responsible for the greater sensitivity to GABA obtained with the fluorescence assay than with the voltage-clamp assay was assessed by repeating the fluorescence experiments with a 2-fold dilution of dye in HEK 293 cells expressing $\alpha1\beta3\gamma2$ (Fig. 3, inset). Under these conditions, the GABA concentration-effect relationship was shifted to the right such that the EC_{50} value (500 nM) was approximately 10-fold higher than with the FMP-Red-Dye dilutions recommended by the supplier (EC_{50}, 40 nM). These results suggest that FMP-Red-Dye acting as a PAM enhances the GABA sensitivity of the fluorescence assay. We found that the 2-fold dilution reduced signal-to-noise and dynamic range and that the assay became unreliable with 5-fold dilution. Therefore, we routinely used FMP-Red-Dye at the dilution recommended by the supplier.

Differential Potencies of Blockers in Cells Expressing Different $GABA_AR$ Isoforms. PTX and TETS are seizure-triggering toxicants that inhibit $GABA_AR$ Cl^- current by binding to overlapping sites within the ion-conducting pore of the channel (Adelsberger et al., 1998; Olsen, 2006; Cao et al., 2012). We sought to demonstrate that the FMP-Red-Dye assay can be used to assess the blocking activity of such agents to validate the assay as a means of identifying novel blockers and quantifying their activity in diverse $GABA_AR$ isoforms. Both PTX and TETS reduced the FMP-Red-Dye signal in HEK 293 cells expressing the $\alpha1\beta3\gamma2$ subunit combination in a concentration-dependent manner, but had negligible influence on $GABA_AR$-null cells (Fig. 4; Table 1). TETS was slightly more potent than PTX (IC_{50} values, 3.8 ± 1.1 and 6.5 ± 1.5 μM, respectively; $P < 0.0001$). Two additional allosteric blockers were tested, TBPS and the insecticide fipronil, and were

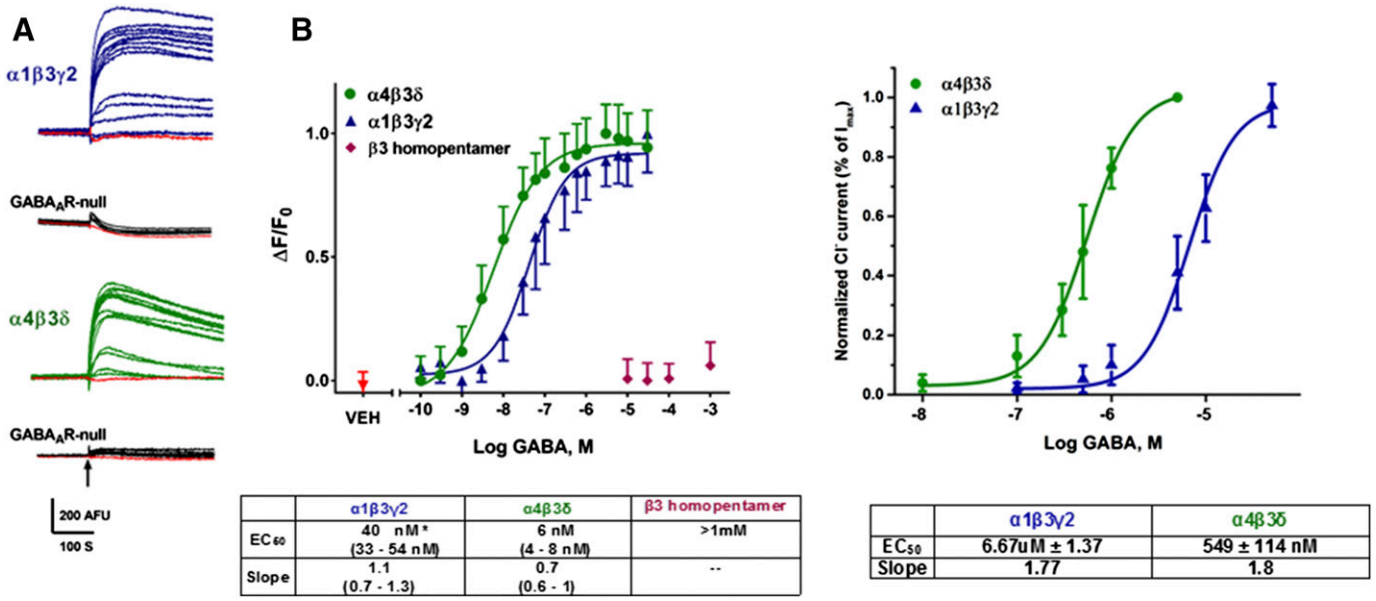

	α1β3γ2	α4β3δ	β3 homopentamer
EC$_{50}$	40 nM* (33 - 54 nM)	6 nM (4 - 8 nM)	>1mM
Slope	1.1 (0.7 - 1.3)	0.7 (0.6 - 1)	--

	α1β3γ2	α4β3δ
EC$_{50}$	6.67uM ± 1.37	549 ± 114 nM
Slope	1.77	1.8

Fig. 3. Comparison of GABA responses in cells expressing GABA$_A$R as assessed with the FMP-Red-Dye technique and by voltage-clamp recording. (A) Both $\alpha1\beta3\gamma2$ and $\alpha4\beta3\delta$ GABA$_A$R-expressing cells exhibit fluorescence responses of increasing amplitude following exposure to increasing concentrations of GABA in the range of 0.1 nM to 30 μM. In these experiments, cells were equilibrated with FMP-Red-Dye for 30 minutes. Then, baseline fluorescence was recorded for 2 minutes followed by exposure to vehicle [(VEH); 0.01% dimethylsulfoxide] or GABA. The $\Delta F/F_0$ values were determined at the peak of the fluorescence response. The black arrow indicates the time of GABA addition; GABA remained for the duration of the recording. GABA$_A$R-null cells do not respond to GABA. (B, left) Concentration-response curves for GABA based on fluorescence responses reveals that $\alpha4\beta3\delta$ GABA$_A$Rs expressed in L-tk cells are significantly more sensitive to GABA than $\alpha1\beta3\gamma2$ GABA$_A$Rs expressed in HEK 293 cells for EC$_{50}$ values of 6 nM [95% confidence interval (CI): 4–8 nM (n_H = 0.7; n = 10)] and 40 nM [95% CI: 33–54 nM (n_H = 1.1; n = 10)]. The $\beta3$ homopentamers transiently expressed in HEK 293 cell are largely insensitive to GABA (EC$_{50}$ > 1 mM). Dose-response curves were plotted using nonlinear regression with a four-parameter logistic equation and independent F test was applied to determine the statistical differences for the EC$_{50}$ values and slopes between $\alpha1\beta3\gamma2$ and $\alpha4\beta3\delta$ GABA$_A$R-expressing cell lines. Each data point represents mean ± S.D. of data from 10 wells. (B, right) Concentration-response curves for GABA activation of $\alpha1\beta3\gamma2$ receptors in HEK 293 cells and $\alpha4\beta3\delta$ receptors in L-tk cells from whole-cell voltage-clamp recordings for EC$_{50}$ values of 6.67 μM [95% CI: 5.30–8.04 μM (n_H = 1.8; n = 13)] and 549 μM [95% CI: 435–663 nM (n_H = 1.8; n = 10] Each data point represents mean ± S.D. *P < 0.0001 for $\alpha1\beta3\gamma2$ versus $\alpha4\beta3\delta$.

shown to have similar potencies to that of TETS (IC$_{50}$ values, 1.8 ± 1.2 and 2.6 ± 1.1 μM, respectively). The GABA$_A$R competitive antagonist bicuculline was approximately 20-times more potent than TBPS (IC$_{50}$ value, 0.1 ± 0.1 μM; P < 0.0001), although its efficacy at reducing fluorescence to that in GABA$_A$R-null cells was less complete at the highest concentration tested (10 μM, data not shown).

L-tk cells expressing $\alpha4\beta3\delta$ subunits showed a distinct structure-activity relationship with the blockers. Although the inhibitory potency of PTX was similar to that in cells expressing $\alpha1\beta3\gamma2$ (IC$_{50}$ values, 6.0 ± 1.0 μM versus 6.5 ± 1.5 μM; P > 0.31), TETS was 2-fold less potent and TBPS and fipronil were nearly 200- and 10-fold more potent at the $\alpha4\beta3\delta$ isoform than at the $\alpha1\beta3\gamma2$ isoform (Table 1).

The divergent potencies exhibited by inhibitors toward cells expressing different GABA$_A$R isoforms compelled us to determine responses of cells expressing only the $\beta3$ subunit, which forms homopentamers that lack high-affinity GABA binding. HEK 293 cells expressing the $\beta3$ homomeric isoform exhibited substantially greater fluorescence than the respective GABA$_A$R-null cells (Fig. 5A), as was the case for the $\alpha1\beta3\gamma2$ isoform (Fig. 4), suggesting that FMP-Red-Dye is able to activate $\beta3$ homomeric GABA$_A$Rs as it does the other isoforms. PTX caused a concentration-dependent inhibition of fluorescence (Fig. 5, C and D) that brought the fluorescence near that in GABA$_A$R-null cells. $\beta3$-Expressing cells failed to response to GABA at concentrations below 1 mM (Fig. 5B), but as in previous voltage-clamp studies (Wooltorton et al., 1997) they did appear to be activated by high (>10 mM) GABA concentrations. Figure 6A shows that hyperpolarization produced by fipronil is also concentration dependent, with fipronil being approximately 10- and 50-fold more potent at restoring E_m values to levels near those measured with GABA$_A$R-null HEK 293 cells than PTX or TETS (Table 1).

Detection of Direct Activation and PAM Activity in GABA$_A$R Isoforms. NAS have been shown to have GABA$_A$R PAM activity at low concentrations and to directly activate GABA$_A$Rs at higher concentrations (Belelli and Lambert, 2005; Wang, 2011). Twenty NAS and related structures were tested for activity on GABA$_A$Rs in the FMP-Red-Dye assay with heterologous cells expressing $\alpha1\beta3\gamma2$, $\alpha4\beta3\delta$, or $\beta3$ homomeric isoforms, and the potency and efficacy of active compounds were quantified (Figs. 7 and 8; Table 2). Several NAS caused concentration-dependent increases in fluorescence in cells expressing the $\alpha1\beta3\gamma2$ and $\alpha4\beta3\delta$ isoforms with EC$_{50}$ values below 1 μM, whereas the respective GABA$_A$R-null cells failed to respond to any NAS. The rank order of potencies (based on the EC$_{50}$ values) in cells expressing the $\alpha1\beta3\gamma2$ isoform was: allopregnanolone/eltanolone/XJ-42 > ganaxolone/3α,21-dihydroxy-5β-preganan-20-one (5β,3α-THDOC)/alphaxalone > alphadolone 21-acetate >> andosterone. Of these, 5β,3α-THDOC and alphadolone 21-acetate showed significantly (P < 0.001) lower efficacy (maximum $\Delta F/F_0$) than the other active NAS (Table 2). By contrast, cells expressing the $\alpha4\beta3\delta$ isoform showed a different rank order of potencies: eltanolone > allopregnanolone > ganaxolone/5β,3α-THDOC/XJ-42/alphaxalone >> alphadolone 21-acetate > androsterone. XJ-42 exhibited significantly greater maximal efficacy in cells expressing

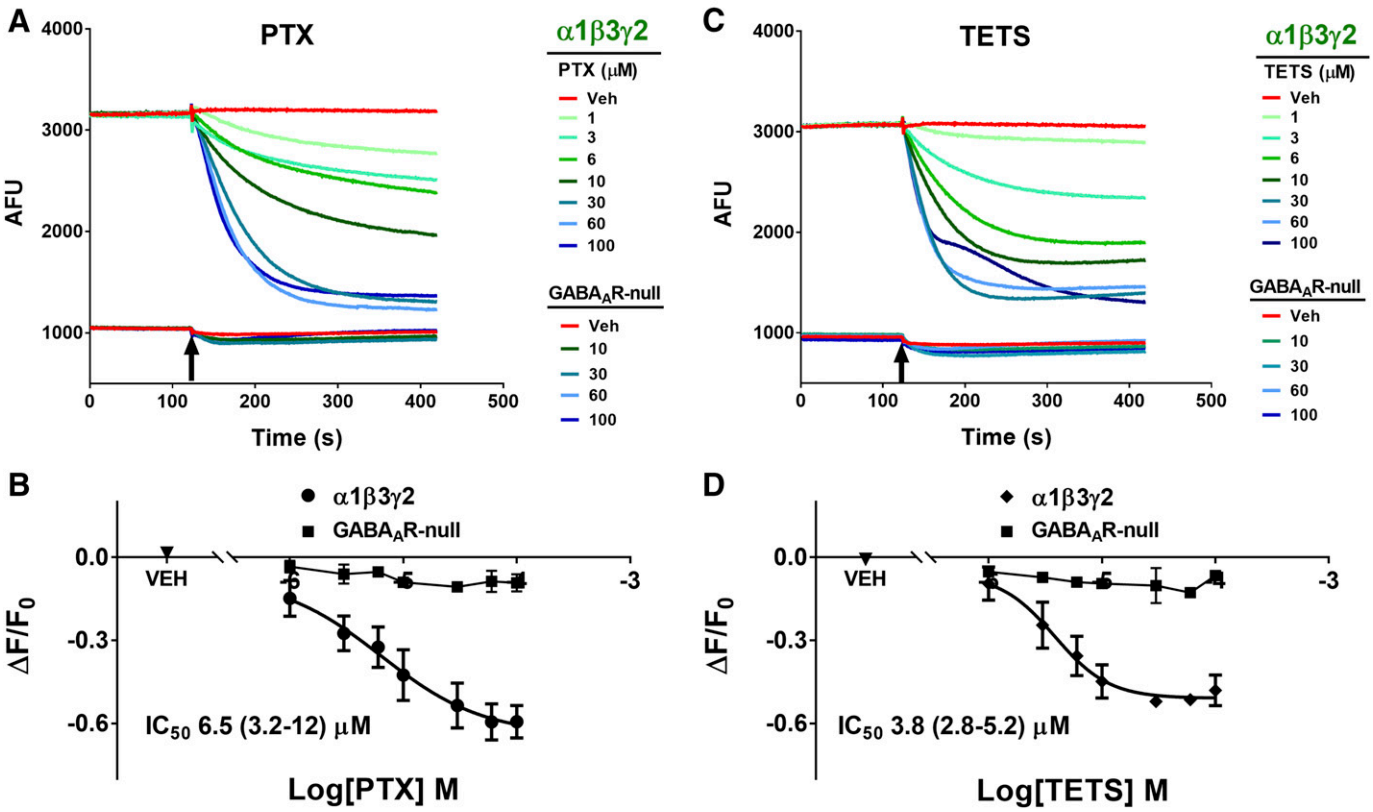

Fig. 4. PTX and TETS block $\alpha_1\beta_3\gamma_2$ $GABA_AR$-dependent FMP-Red-Dye fluorescence. HEK 293 cells stably transfected with $\alpha1\beta3\gamma2$ $GABA_AR$ were exposed to FMP-Red-Dye for 30 minutes to activate the receptors. $GABA_AR$-null cells were used as the control. PTX (A) or TETS (C) caused slow, concentration-dependent inhibition of the fluorescence in cells expressing $\alpha1\beta3\gamma2$ $GABA_AR$; minimal effects were obtain in $GABA_AR$-null cells. Arrows indicate time of addition of PTX and TETS to the wells; the blockers were not removed. (B and D) Plots of $\Delta F/F_0$ from experiments similar to those illustrated in (A) and (C). Each plot represents eight experiments. The IC_{50} values are 6.5 μM [95% confidence interval (CI): 3.2–12 μM] and 3.8 μM (95% CI: 2.8–5.2 μM) for PTX and TETS, respectively. TETS is significantly more potent than PTX ($P < 0.0001$). Dose-response curves were plotted using nonlinear regression with a four-parameter logistic equation and independent F test was applied to determine the statistical differences for the EC_{50} values between TETS and PTX. Each data point represents mean ± S.D. of data from eight wells. Red traces represent responses to vehicle (0.01% dimethylsulfoxide). *$P < 0.0001$.

$\alpha4\beta3\delta$ ($P < 0.007$) than the other active NAS, whereas 5β,3α-THDOC had significantly lower efficacy (Figs. 7E and 8E; Table 2). Overall, with the exception of eltanolone, all active NAS were modestly more potent on $\alpha1\beta3\gamma2$ than $\alpha4\beta3\delta$ ($P < 0.0038$). In contrast to other isoforms, $\beta3$ homopentameric channels were insensitive to allopregnanolone (Fig. 6B) and in general to all NAS tested (data not shown).

We next tested whether the FMP-Red-Dye assay is able to detect the PAM activity of NAS and exposed cells to a low, submaximal concentration of GABA (10 nM) with and without various concentrations of NAS. Figure 9A plots the fold increase in fluorescence signal in HEK 293 cells expressing the $\alpha1\beta3\gamma2$ isoform in the presence of allopregnanolone or ganaxolone compared with the signal elicited by GABA alone. The EC_{50}

TABLE 1

Potencies of blockers on $\alpha1\beta3\gamma2$, $\alpha4\beta3\delta$, and $\beta3$ homopentamer $GABA_AR$ isoforms as assessed using the FMP-Red-Dye fluorescence assay

Dose-response curves were plotted using nonlinear regression with a four-parameter logistic equation. Separate one-way analysis of variance with additional correction (Tukey) for post hoc multiple comparisons was applied for EC_{50} and slope to determine the statistical differences among them. The IC_{50} values and slopes were compared within each receptor isoform. On $\alpha1\beta3\gamma2$ $GABA_A$Rs, bicuculline is significantly more potent than the other blockers; the IC_{50} values of the other blockers were not significantly different from each other. On $\alpha4\beta3\delta$ $GABA_A$Rs, TBPS and fipronil are significantly more potent than the other blockers. The slope values for PTX and TETS are significantly smaller than for the other blockers. On $\beta3$ homopentamer, fipronil is more potent than PTX and TETS. The slope for fipronil is significantly smaller than that of PTX and TETS. Each data point represents the mean (with 95% confidence interval in parenthesis) of measurements in eight wells. *$P < 0.001$ when comparing IC_{50} values or slopes of blockers within each receptor isoform.

Isoform	PTX	TETS	TBPS	Fipronil	Bicuculline
$\alpha1\beta3\gamma2$					
IC_{50} (95% CI)	6.5 μM * (3.2–12 μM)	3.8 μM (2.8–5.2 μM)	1.8 μM (1.1–2.9 μM)	2.6 μM (1.6–3.6 μM)	0.1 μM * (0.03–0.8)
Slope (95% CI)	−1.0 (−1.7 to −0.1)	−1.8 (−2.6 to −0.9)	−0.7 * (−0.8 to −0.5)	−0.8 (−1 to −0.7)	−1 (−1.4 to −0.3)
$\alpha4\beta3\delta$					
IC_{50}	6 μM (2.9–13 μM)	7 μM (4–15 μM)	0.01 μM * (0.009–0.015 μM)	0.25 μM * (0.14–0.5 μM)	7 μM (6.8–9 μM)
Slope	−0.1 (−0.2 to −0.07)	−0.1 (−0.3 to −0.04)	−1 * (−1.2 to −0.7)	−0.40 * (−0.7 to −0.1)	−1 * (−1.5 to −0.5)
$\beta3$ homopentamer					
IC_{50}	1.8 μM * (1.4–2.2 μM)	10 μM (8.6–11 μM)	Not tested	0.2 μM * (0.1–0.9 μM)	Not tested
Slope	−1.7 (−2.2 to −1.2)	−2.1 (−2.7 to −1.4)	Not tested	−0.6 * (−0.8 to −0.3)	Not tested

CI, confidence interval.

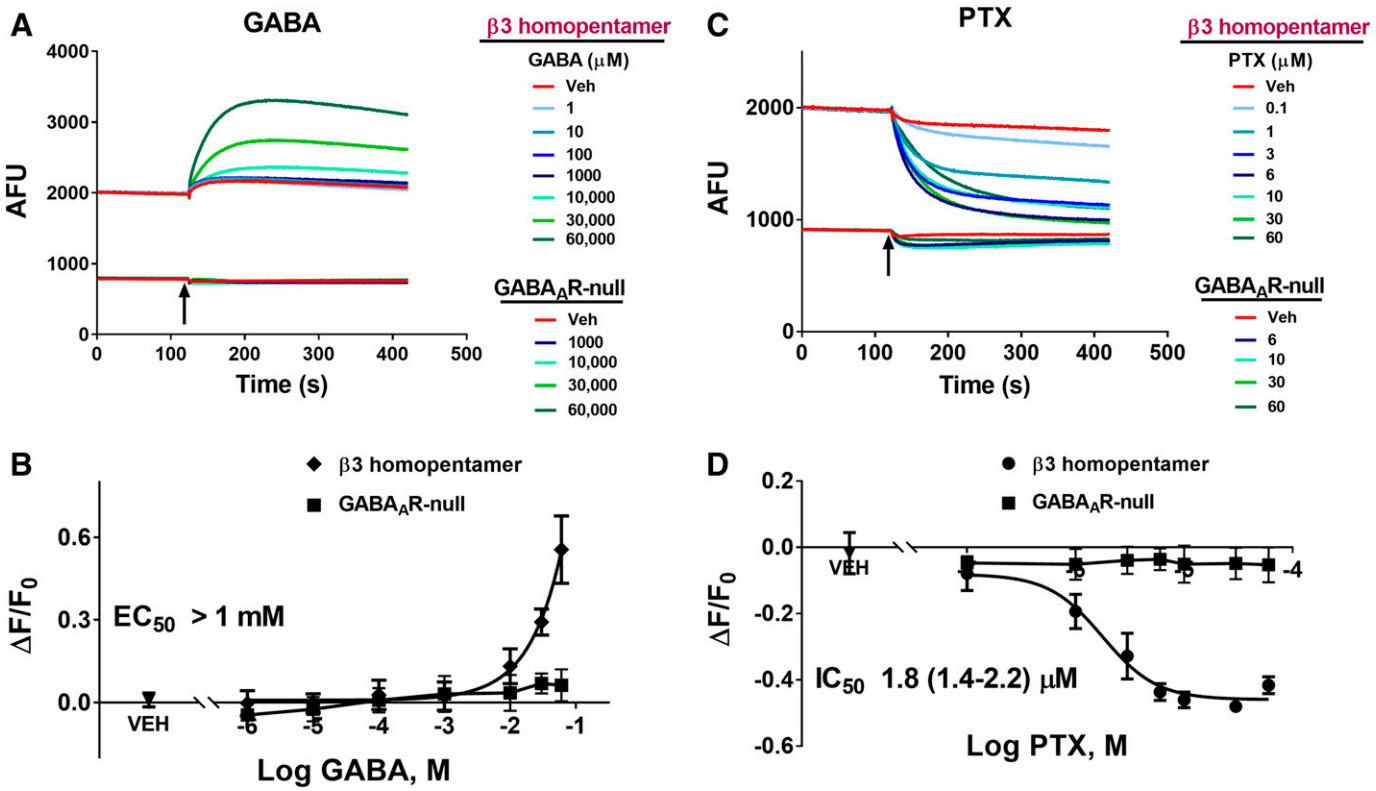

Fig. 5. GABA potentiation and PTX inhibition of β_3 homopentameric GABA$_A$R-dependent FMP-Red-Dye fluorescence. HEK 293 cells transiently transfected with β3 homopentameric GABA$_A$R were exposed to FMP-Red-Dye for 30 minutes to activate the receptors. GABA$_A$R-null cells were used as the control. (A) GABA caused slow, concentration-dependent potentiation of the fluorescence in cells expressing β3 homopentameric GABA$_A$R; minimal effects were obtained in GABA$_A$R-null cells. (B) PTX caused slow, concentration-dependent inhibition of the fluorescence in cells expressing β3 homopentameric GABA$_A$R; minimal effects were obtained in GABA$_A$R-null cells. Arrows indicate time of addition of GABA and PTX, which was not removed. Red traces represent the responses to vehicle (0.01% dimethylsulfoxide). (B and D) Plots of $\Delta F/F_0$ from experiments similar to those illustrated in (A) and (C). Each data point represents mean ± S.D. of data from 10 wells. The EC$_{50}$ value for GABA could not be determined since the response did not plateau. The IC$_{50}$ value for PTX is 1.8 μM (95% confidence interval: 1.4–2.2 μM). Dose-response curves were plotted for PTX using nonlinear regression with a four-parameter logistic equation.

values for the two NAS are 1.7 ± 1.2 nM (n_H = 1.49) and 20 ± 13 nM (n_H = 1.43), respectively. Because GABA$_A$R channel opening probability increases and maximizes with increasing GABA concentrations, the relative increase in response by a PAM will necessarily drop in magnitude as the GABA concentration is increased. This is demonstrated in the experiment shown in Supplemental Fig. 3. The relative enhancement produced by 1 nM allopregnanolone in the presence of 1, 10, and 100 nM GABA is greatest at the lowest GABA concentration, reduced at 10 nM GABA, and there is no further enhancement with 100 nM GABA, which is a near saturating GABA concentration in the FMP-Red-Dye assay (Fig. 3B). Results from voltage-clamp experiments demonstrating the PAM effect with transiently expressed $\alpha1\beta3\gamma2$ GABA$_A$Rs are shown in Fig. 9B. Addition of allopregnanolone or ganaxolone in the presence of the GABA EC$_{10}$ values (1 μM) (Fig. 3B) caused concentration-dependent enhancement of the Cl^- current with EC$_{50}$ values of 71.7 ± 14.2 nM (n_H = 1.8) and 114.8 ± 15.6 nM (n_H = 2.2), respectively.

Finally, we tested whether the FMP-Red-Dye assay could detect direct or PAM effects of the benzodiazepine midazolam.

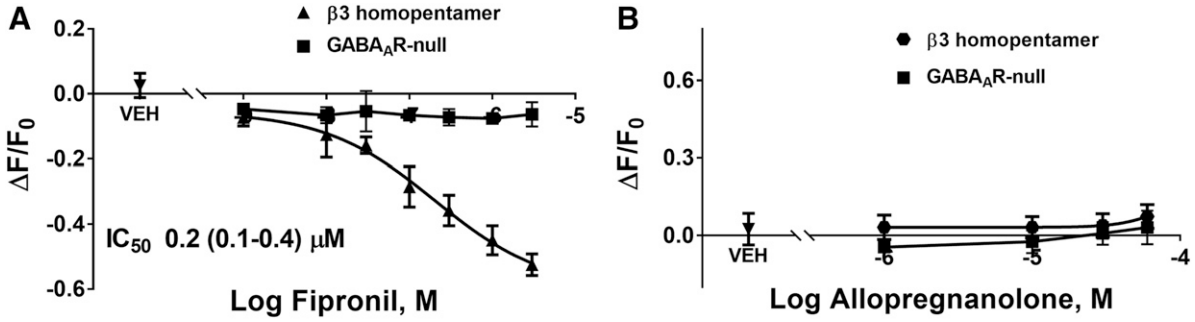

Fig. 6. Fipronil blocks β3-homomeric GABA$_A$Rs, while allpregnanolone fails to affect the fluorescence signal even at concentrations ≥ 10 μM. (A) Fipronil blocks β3 receptors in a concentration-dependent manner but does not have any significant effects on GABA$_A$R-null cells. Dose-response curves were plotted using nonlinear regression with a four-parameter logistic equation. Each data point represents mean ± S.D. of data from eight wells. (B) Allopregnanolone does not have any effect even at 10 μM.

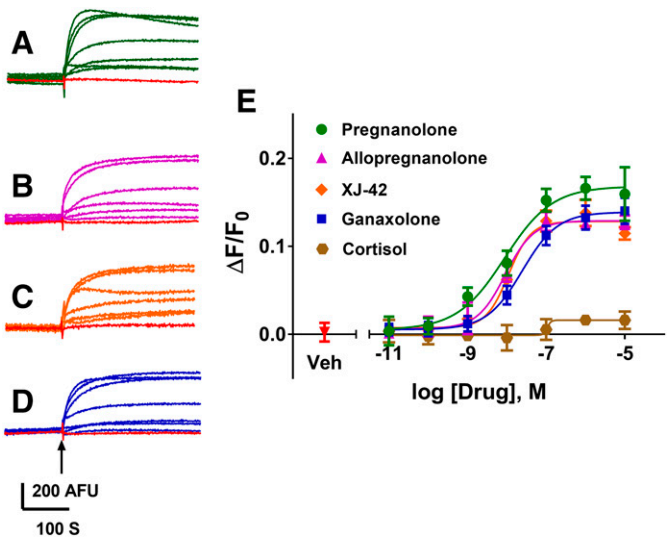

Fig. 7. NAS-induced FMP-Red-Dye fluorescence responses of $\alpha1\beta3\gamma2$ $GABA_AR$ in HEK 293 cells. (A–D) Representative traces of responses to 0.01 nM to 10 μM of eltanolone, allopregnanolone, XJ-42, and ganaxolone, respectively. The arrow indicates time of addition of the test compound, which was not removed. Red traces represent the responses to vehicle (0.01% dimethylsulfoxide). (E) Concentration-response curves for each NAS and cortisol. Dose-response curves were plotted using nonlinear regression with a four-parameter logistic equation. Separate one-way analysis of variance with additional correction (Tukey) for post hoc multiple comparisons was applied for EC_{50} and slope to determine the statistical differences within a subunit composition—not across subtypes (Table 2). Each data point represents mean ± S.D. of data from 10 wells.*$P < 0.0001$.

In the absence of GABA, midazolam failed to substantially enhance the fluorescence signal in HEK 293 cells expressing the $\alpha_1\beta_3\gamma_2$ isoform at concentrations ≤ 1 μM, although at higher concentrations a small signal was elicited (Fig. 10). In the presence of suboptimal GABA (10 nM), midazolam caused a concentration-dependent increase in fluorescence signal with EC_{50} values of 51 ± 12 nM (Fig. 10).

Discussion

The present results demonstrate that FMP-Red-Dye, which contains the fluorescent voltage-sensor $DiSBAC_1(3)$, can be used with the FLIPR platform to characterize a wide range of $GABA_AR$ blockers and modulators in heterologously expressed recombinant $GABA_ARs$. However, because FMP-Red-Dye interacts with $GABA_ARs$, causing a PAM effect, quantitative results obtained with the potentiometric dye approach may not correspond to results obtained with other methods, such as the gold standard voltage-clamp technique. The potentiometric indicator $DiSBAC_1(3)$ is a thiobarbiturate. Compared with other potentiometric dyes in the family of oxonol slow indicators, DiSBAC indicators have been reported to have reduced direct activating and PAM influences on $GABA_ARs$ compared with BiBAC dyes (Mennerick et al., 2010). Our present data indicate that $DiSBAC_1(3)$ is a relatively weak direct activator of $GABA_AR$-mediated Cl^- currents in the absence of GABA or UV irradiation, but as previously reported for oxonols, UV irradiation greatly potentiates this activity. Equilibration of HEK 293 or L-tk cells that express $GABA_ARs$ with FMP-Red-Dye in the dark results in a modest chronic depolarization of resting E_m regardless of $GABA_AR$ isoform expression compared with respective $GABA_AR$-null cells. Depolarization of cells expressing $GABA_ARs$ by FMP-Red-Dye is likely the direct consequence of interactions of the dye molecules at barbiturate sites localized within membrane spanning regions of the β subunit to directly activate Cl^- current (Löscher and Rogawski, 2012).

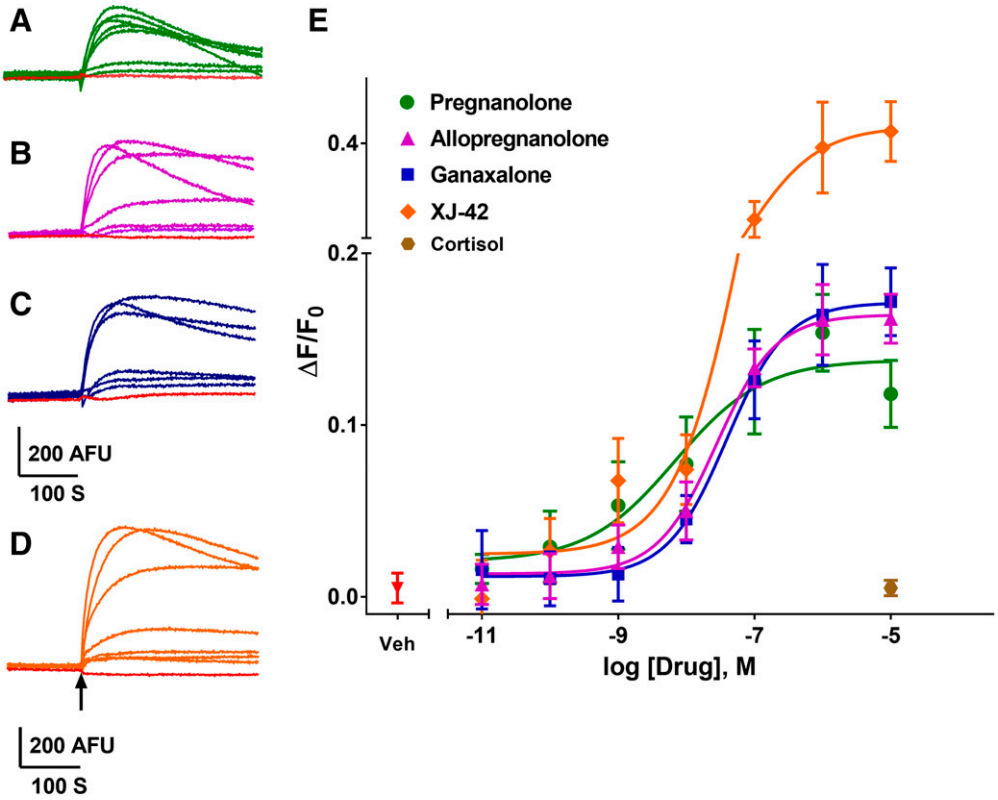

Fig. 8. NAS-induced FMP-Red-Dye fluorescence responses of $\alpha4\beta3\delta$ $GABA_ARs$ in L-tk cells. (A–D) Representative traces of responses to 0.01 nM to 10 μM of eltanolone, allopregnanolone, XJ-42, and ganaxolone, respectively. The arrow indicates time of addition of the test compound, which was not removed. Red traces represent the responses to vehicle (0.01% dimethylsulfoxide). (E) Concentration-response curves for each NAS. Dose-response curves were plotted using nonlinear regression with a four-parameter logistic equation. Separate one way analysis of variance with additional correction (Tukey) for post hoc multiple comparisons was applied for EC_{50} and slope to determine the statistical differences within a subunit composition—not across subtypes (Table 2). Each data point represents mean ± S.D. of data from 10 wells.*$P < 0.0001$.

TABLE 2

EC_{50} and maximum $\Delta F/F_0$ values (95% confidence interval in the parenthesis) for NAS and related compounds and benzodiazepines to increase FMP-Red-Dye flourescence in cells expressing $\alpha1\beta3\gamma2$ and $\alpha4\beta3\delta$ $GABA_AR$ in the absence of GABA

Dose-response curves were fit by nonlinear regression with a four-parameter logistic equation. Statistical differences among EC_{50} and maximum $\Delta F/F_0$ values were assessed independently by one-way analysis of variance with post hoc pairwise comparisons using Tukey's honest significant difference test. On $\alpha1\beta3\gamma2$ $GABA_ARs$, eltanolone with an IC_{50} value of 8 nM and maximum of 0.17 is the most potent and efficacious compound. Although on $\alpha4\beta3\delta$ $GABA_ARs$, eltanolone with an IC_{50} value of 6 nM is the most potent compound, and XJ-42 with a maximum of 0.41 is the most efficacious compound. Each data point represents the mean (with 95% confidence interval in parenthesis) of measurements in 10 wells. *$P < 0.001$ when comparing IC_{50} values or maximum of compounds within each receptor isoform.

Compound Common Name (Systematic Name)	$\alpha1\beta3\gamma2$ (95% CI)		$\alpha4\beta3\delta$ (95% CI)	
	EC_{50}	Maximum $\Delta F/F_0$	EC_{50}	Maximum $\Delta F/F_0$
Allopregnanolone (3α-hydroxy-5α-pregnan-20-one)	9 nM * (7–11 nM)	0.13 (0.12–0.13)	27 nM (18–42 nM)	0.16 (0.15–0.17)
Ganaxolone (3α-hydroxy-3β-methyl-5α-pregnan-20-one)	24 nM (18–32 nM)	0.14 (0.13–0.14)	40 nM (21–73 nM)	0.17 (0.15–0.18)
Eltanolone (3α-hydroxy-5β-pregnan-20-one)	8 nM * (5–14 nM)	0.17 * (0.16–0.18)	6 nM * (2.4–16 nM)	0.14 (0.12–0.15)
XJ-42 (3α,5α,20E)-3-hydroxy-13,24-cyclo-18-norcholan-20-ene-21-carbonitrile)	11 nM * (7–17 nM)	0.13 (0.12–0.14)	74 nM (47–116 nM)	0.41 * (0.38–0.45)
5β,3α-THDOC (5β-pregnan-3α,21-diol-20-one)	16 nM (6–45 nM)	0.09 (0.08–0.10)	54 nM (12–230 nM)	0.09 (0.06–0.12)
Alphadolone 21-acetate (5α-pregnan-3α,21-diol-11, 20-dione 21-acetate)	60 nM (33–100 nM)	0.08 (0.07–0.09)	700 nM (381–1220 nM)	0.14 (0.1–0.18)
Alphaxalone ((3α,5α)-3-hydroxypregnane-11,20-dione)	26 nM (13–54 nM)	0.11 (0.10–0.11)	83 nM (72–97 nM)	0.13 (0.11–0.15)
Androsterone (5α-androstan-3α-ol-17-one)	300 nM (200–551 nM)	0.16 * (0.14–0.18)	>1 μM	
Etiocholanolone (5β-androstan-3α-ol-17-one)	>1 μM		>5 μM	
Org 20599 ((2β,3α,5α)-21-chloro-3-hydroxy-2-(4-morpholinyl)pregnan-20-one)	>1 μM		>1 μM	
UCI-50027 (3-[3α-hydroxy-3β-methyl-5α-androstan-17β-yl]-5(hydroxymethyl)isoxazole)	>5 μM		>5 μM	
Progesterone (pregn-4-ene-3,20-dione)	>5 μM		>5 μM	
Epiandrosterone (5α-androstan-3β-ol-17-one)	>5 μM		>5 μM	
Indiplon (*N*-methyl-*N*-[3-[3-(2-thienylcarbonyl) pyrazolo[1,5-α]pyrimidin-7-yl]phenyl]-acetamide)	>5 μM		>5 μM	
Androstenediol (5-Androsten-3β, 17β-diol)	>5 μM		>5 μM	
Dehydroepiandrosterone (DHEA) acetate	>5 μM		>10 μM	
Dehydroepiandrosterone (DHEA)	>5 μM		Inactive	
20α-Dihydropregnenolone (5-pregnen-3β,20α-diol)	>10 μM		>10 μM	
Ursodeoxycholic acid (sodium salt) (3,7-dihydroxy-cholan-24-oic acid, monosodium salt)	Inactive		Inactive	
Cortisol (4-pregnen-11β,17,21-triol-3,20-dione)	Inactive		Inactive	
Diazepam (7-chloro-1-methyl-5-phenyl-1,3-dihydro-2*H*-1,4-benzodiazepin-2-one)	>10 μM		>10 μM	
Midazolam (8-chloro-6-(2-fluorophenyl)-1-methyl-4*H*-imidazo[1,5-a][1,4]benzodiazepine)	>10 μM		>10 μM	
Zolpidem (*N*,*N*,6-trimethyl-2-(4-methylphenyl)-imidazo[1,2-a]pyridine-3-acetamide)	>10 μM		>10 μM	

CI, confidence interval.

In the case of our HEK 293 or L-tk cell expression models, the electrochemical gradient for chloride causes an inward current (outward Cl^- flux) that results in depolarization when $GABA_AR$ channel opening is increased and hyperpolarization when channel opening is decreased, consistent with the voltage-clamp measurements here and those of others in such cell types. This interpretation is supported by the experimental findings with channel blockers, including PTX, TETS, and fipronil, that bring the fluorescence signal back to levels near those measured in the respective $GABA_AR$-null cells.

It is noteworthy that in both the potentiometric and voltage-clamp assays, GABA was ~10-fold more potent as an activator of the extrasynaptic subunit combination $\alpha4\beta3\delta$ than of the synaptic subunit combination $\alpha1\beta3\gamma2$, while $\beta3$ homopentamers were insensitive to GABA ($\leq$1 mM). These differences in GABA sensitivity are in accord with previous reports (Brickley and Mody, 2012; Mortensen et al., 2012). For both the synaptic and extrasynaptic subunit combinations, GABA potency in the FMP-Red-Dye assay was two orders of magnitude greater than in patch-clamp experiments. A review of the available electrophysiological literature indicates that conventional barbiturates, such as pentobarbital, induce a more modest 3- to 10-fold leftward shift in sensitivity to GABA (Steinbach and Akk, 2001; Löscher and Rogawski, 2012). The basis for the extreme GABA sensitivity in the FMP-Red-Dye assay is not fully understood but could relate to the fact that the $DiSBAC_1(3)$ molecule contains two thiobarbiturate moieties, which could interact with mutiple sites on $GABA_ARs$ thus acting as synergistic positive modulators. Whatever the cause of the high sensitivity to GABA, the FMP-Red-Dye FLIPR platform provides an extremely sensitive assay for detecting and quantifying responses to $GABA_AR$ agonists, antagonists, and modulators on defined $GABA_AR$ subtypes.

Two new findings emerge from studies with the potentiometric assay. First, the rank order of potencies of noncompetitive $GABA_AR$ blockers toward $\alpha1\beta3\gamma2$ (TBPS > TETS/fipronil > PTX) differs from that of $\alpha4\beta3\delta$ (TBPS >> fipronil >> TETS/PTX). Second, the approximately 10- and 100-fold higher potencies of fipronil and TBPS toward blocking the basal activity (i.e., normalizing E_m in the absence of GABA) of cells expressing the extrasynaptic $\alpha4\beta3\delta$ combination compared with either of those that express the synaptic $\alpha1\beta3\gamma2$ combination or $\beta3$ homopentamers is particularly noteworthy in that it suggests for the first time that blockers with both compact and elongated chemical structures (Zhao et al., 2014) selectively target major extrasynaptic $GABA_ARs$ within the mammalian central nervous system, albeit with TBPS having 25-fold higher potency than fipronil (see Table 1). We also note that fipronil is substantially more potent than either PTX or TETS (10- and 50-fold, respectively)

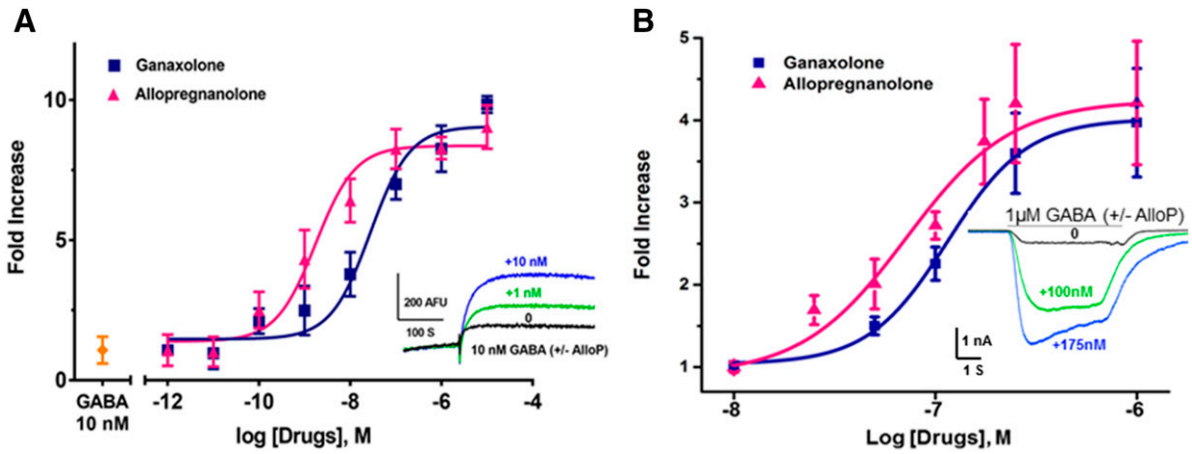

Fig. 9. Allopregnanolone and ganaxolone potentiation of GABA responses of $\alpha1\beta3\gamma2$ $GABA_AR$ in HEK 293 cells. (A) Concentration-response curves for allopregnanolone and ganaxolone potentiation of FMP-Red Dye responses to 10 nM GABA. The graph plots mean ± S.D. fold increase in peak response in the presence the NAS compared with the response to 10 nM GABA alone. Each data point is the mean ± S.D. of measurements of 10 wells. The EC_{50} values for allopregnanolone and ganaxolone are 1.7 nM [95% confidence interval (CI): 1–3.1 nM (n_H = 1.5)] and 20 nM [95% CI: 14–55 nM (n_H = 1.4)], respectively ($P < 0.0001$). Dose-response curves were plotted using nonlinear regression with a four-parameter logistic equation and independent F test was applied to determine the statistical differences for EC_{50} values and slopes between allopregnanolone and ganaxolone in combination with 10 nM GABA in $\alpha1\beta3\gamma2$ $GABA_AR$ in HEK 293 cells. Inset shows representative traces with addition of GABA alone and GABA plus allopregnanolone at concentrations of 1 and 10 nM. (B) Concentration-response curves for allopregnanolone and ganaxolone potentiation of peak inward Cl^- current responses to 1 μM GABA (EC_{10} value) in patch-clamp recordings. Each data point is the mean ± S.D. of measurements of 3–6 cells. The EC_{50} values for allopregnanolone and ganaxolone are 71.3 nM [95% CI: 57.1–85.5 nM (n_H = 1.8)] and 114.8 nM [95% CI: 99.2–130.4 nM (n_H = 2.2)], respectively. Inset shows representative traces with application of GABA alone and GABA plus allopregnanolone at 100 and 175 nM.

toward $\beta3$ homopentamers, as previously demonstrated in receptor binding studies (Chen et al., 2006; Zhao et al., 2014). The findings identifying differential potencies of blockers toward synaptic and extrasynaptic $GABA_AR$ subunit combinations could help explain outstanding questions with respect to toxicological mechanisms, including the pharmacodynamic basis for the different seizure-inducing potencies of different $GABA_AR$ blockers. In addition, if it is the case that TBPS and fipronil are generally more active at extrasynaptic $GABA_AR$ subunit combinations, these agents may be useful as pharmacological tools for selectively blocking these receptors. The competitive $GABA_AR$ antagonist bicuculline was the most potent blocker of the $\alpha1\beta3\gamma2$ isoform that we studied. However, it failed to completely reduce the fluorescence to that in $GABA_AR$-null cells, a result fully in accord with previous voltage-clamp studies where high concentrations of bicuculline fully block GABA-activated Cl^- current but not barbiturate-activated current (Rho et al., 1996). Interestingly, bicuculline exhibited the opposite relative selectivity to that of TBPS and fipronil inasmuch as the $\alpha4\beta3\delta$ isoform was less sensitive than the $\alpha1\beta3\gamma2$ isoform.

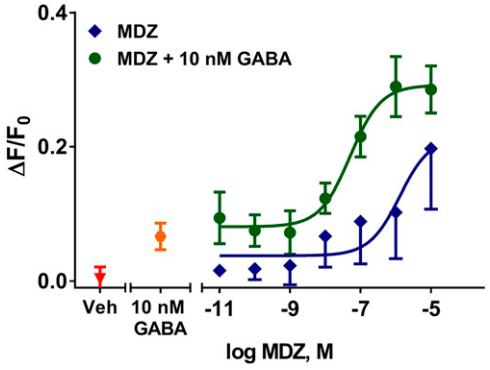

Fig. 10. Effects of midazolam on FMP-Red-Dye fluorescence in cells expressing $\alpha1\beta3\gamma2$ $GABA_AR$. In the absence of GABA, midazolam fails to generate substantial fluorescence signals compared with vehicle (Veh) except at high concentrations (>1 μM). GABA (10 nM) induces a small fluorescence signal. Combination of midazolam and GABA results in potentiation of the signal [EC_{50}, 51 nM (95% confidence interval: 30–83 nM)]. Dose-response curves were plotted using nonlinear regression with a four-parameter logistic equation. Each data point represents the mean ± S.D. of measurements in eight cells.

The FMP-Red-Dye potentiometric assay proved to be an excellent system for characterizing both the directly activating and the PAM effects of NAS. Of the 20 NAS tested, only eight activated $GABA_AR$ with potencies (EC_{50} values) below 1 μM (Table 2). In general, the structure-activity relationship that emerges from the FMP-Red-Dye assay is consistent with previous reports in the literature (Kokate et al., 1994; Akk et al., 2007; Borowicz et al., 2011; Wang, 2011; Reddy and Rogawski, 2012). Both synaptic and extrasynaptic $GABA_AR$ subtypes respond to NAS (Bianchi and Macdonald, 2003; Maksay et al., 2000). In general, we found comparable potencies (EC_{50} values) and efficacies ($\Delta F/F_0$ values) of the active steroids at the synaptic $\alpha1\beta3\gamma2$ isoform and the extrasynaptic $\alpha4\beta3\delta$ isoform. In contrast to the other active steroids that all had similar maximal efficacies, XJ-42, a pentacyclic analog of allopregnanolone with a 17,18-fused carbonitrile-substituted 6-member carbocyclic ring, had substantially greater efficacy although its potency was in line with that of the other active steroids. This observation indicates that modifications that replace the 17-acetyl group of allopreganolone can enhance NAS efficacy, which may provide therapeutic advantages. In addition to directly activating $GABA_ARs$, at low concentrations NAS act as PAMs to enhance the action of GABA (Kokate et al., 1994). The FMP-Red-Dye assay is able to demonstrate such an effect as illustrated in Fig. 9A, which compares the PAM activity of allopregnanolone and ganaxolone, two exemplary NAS currently under clinical investigation (Reddy and Rogawski, 2012). In experiments with the synaptic $\alpha1\beta3\gamma2$ combination, both steroids exhibit substantial PAM activity in the FMP-Red-Dye assay, with allopregnanolone demonstrating modestly

greater potency than ganaxolone. Similar relative potencies were obtained in patch-clamp recordings (Fig. 9B) (see Carter et al., 1997). Because of the heightened sensitivity to GABA due to the influence of FMP-Red-Dye, the PAM activity of NAS was measured in the presence of a low concentration GABA (10 nM) to prevent saturation evident even at 100 nM GABA (Supplemental Fig. 3). Under these conditions, the FMP-Red-Dye assay generates EC_{50} and fold-increase values that indicate substantially greater potency and efficacy than obtained with electrophysiological methods, but the relative potencies are consistent with previous reports using receptor binding and electrophysiological methods (Carter et al., 1997).

Conclusions

FMP-Red-Dye–based assays provide sensitive and quantitative approaches to investigate functional interactions with $GABA_AR$ subtypes mediated through the GABA site, PAM sites, or channel pore sites. FMP-Red-Dye is useful not only for discovery of antiseizure drugs but also for identifying novel channel blockers of interest to insecticide discovery or biosecurity.

Authorship Contributions

Participated in research design: Nik, Hulsizer, Wulff, Pessah.

Conducted experiments: Nik, Pressly, Singh, Antrobus.

Contributed new reagents or analytic tools: Rogawski, Wulff, Pessah.

Performed data analysis: Nik, Pressly, Singh, Hulsizer, Wulff, Pessah.

Wrote or contributed to the writing of the manuscript: Nik, Pressly, Singh, Antrobus, Hulsizer, Rogawski, Wulff, Pessah.

References

Adelsberger H, Brunswieck S, and Dudel J (1998) Block by picrotoxin of a GABAergic chloride channel expressed on crayfish muscle after axotomy. *Eur J Neurosci* **10**: 179–187.

Akabas MH (2004) $GABA_A$ receptor structure-function studies: a reexamination in light of new acetylcholine receptor structures. *Int Rev Neurobiol* **62**:1–43.

Akk G, Covey DF, Evers AS, Steinbach JH, Zorumski CF, and Mennerick S (2007) Mechanisms of neurosteroid interactions with $GABA_A$ receptors. *Pharmacol Ther* **116**:35–57.

Alvarez LD and Estrin DA (2015) Exploring the molecular basis of neurosteroid binding to the $\beta3$ homopentameric $GABA_A$ receptor. *J Steroid Biochem Mol Biol* **154**:159–167.

Barnard EA, Skolnick P, Olsen RW, Mohler H, Sieghart W, Biggio G, Braestrup C, Bateson AN, and Langer SZ (1998) International Union of Pharmacology. XV. Subtypes of γ-aminobutyric $acid_A$ receptors: classification on the basis of subunit structure and receptor function. *Pharmacol Rev* **50**:291–313.

Belelli D, Harrison NL, Maguire J, Macdonald RL, Walker MC, and Cope DW (2009) Extrasynaptic $GABA_A$ receptors: form, pharmacology, and function. *J Neurosci* **29**: 12757–12763.

Belelli D and Lambert JJ (2005) Neurosteroids: endogenous regulators of the $GABA_A$ receptor. *Nat Rev Neurosci* **6**:565–575.

Bettler B and Tiao JY (2006) Molecular diversity, trafficking and subcellular localization of $GABA_B$ receptors. *Pharmacol Ther* **110**:533–543.

Bianchi MT and Macdonald RL (2003) Neurosteroids shift partial agonist activation of $GABA_A$ receptor channels from low- to high-efficacy gating patterns. *J Neurosci* **23**:10934–10943.

Borowicz KK, Piskorska B, Banach M, and Czuczwar SJ (2011) Neuroprotective actions of neurosteroids. *Front Endocrinol (Lausanne)* **2**:50.

Braat S and Kooy RF (2015) The $GABA_A$ receptor as a therapeutic target for neurodevelopmental disorders. *Neuron* **86**:1119–1130.

Brickley SG and Mody I (2012) Extrasynaptic $GABA_A$ receptors: their function in the CNS and implications for disease. *Neuron* **73**:23–34.

Brodie JM, Besag F, Ettinger BA, Mula M, Gobbi G, Comai S, Aldenkamp PA, and Steinhoff JB (2016) Epilepsy, Antiepileptic Drugs, and Aggression: An Evidence-Based Reviews. *Pharmacol Rev* **68**:563–602.

Brown N, Kerby J, Bonnert TP, Whiting PJ, and Wafford KA (2002) Pharmacological characterization of a novel cell line expressing human $\alpha_4\beta_3\delta$ $GABA_A$ receptors. *Br J Pharmacol* **136**:965–974.

Campagna-Slater V and Weaver DF (2007) Molecular modelling of the $GABA_A$ ion channel protein. *J Mol Graph Model* **25**:721–730.

Cao Z, Hammock BD, McCoy M, Rogawski MA, Lein PJ, and Pessah IN (2012) Tetramethylenedisulfotetramine alters Ca^{2+} dynamics in cultured hippocampal neurons: mitigation by NMDA receptor blockade and $GABA_A$ receptor-positive modulation. *Toxicol Sci* **130**:362–372.

Carter RB, Wood PL, Wieland S, Hawkinson JE, Belelli D, Lambert JJ, White HS, Wolf HH, Mirsadeghi S, Tahir SH, et al. (1997) Characterization of the anticonvulsant properties of ganaxolone (CCD 1042; 3α-hydroxy-3β-methyl-5α-pregnan-20-one), a selective, high-affinity, steroid modulator of the γ-aminobutyric $acid_A$ receptor. *J Pharmacol Exp Ther* **280**:1284–1295.

Casida JE and Durkin KA (2015) Novel GABA receptor pesticide targets. *Pestic Biochem Physiol* **121**:22–30.

Chen L, Durkin KA, and Casida JE (2006) Structural model for γ-aminobutyric acid receptor noncompetitive antagonist binding: widely diverse structures fit the same site. *Proc Natl Acad Sci USA* **103**:5185–5190.

Chen ZW, Manion B, Townsend RR, Reichert DE, Covey DF, Steinbach JH, Sieghart W, Fuchs K, and Evers AS (2012) Neurosteroid analog photolabeling of a site in the third transmembrane domain of the $\beta3$ subunit of the $GABA_A$ receptor. *Mol Pharmacol* **82**:408–419.

Covey DF and Jiang X (2014) inventors, Washington University, assignee. Neuroactive 13,24-cyclo-18,21-dinorcholanes and structurally related pentacylic steroids. U.S. Patent 8,759,330. 2014 Jun 24.

Dasheiff RM (1985) A new method of monitoring membrane potential in rat hippocampal slices using cyanine voltage-sensitive dyes. *J Neurosci Methods* **13**: 199–212.

Fairless R, Beck A, Kravchenko M, Williams SK, Wissenbach U, Diem R, and Cavalié A (2013) Membrane potential measurements of isolated neurons using a voltage-sensitive dye. *PLoS One* **8**:e58260.

Herd MB, Belelli D, and Lambert JJ (2007) Neurosteroid modulation of synaptic and extrasynaptic $GABA_A$ receptors. *Pharmacol Ther* **116**:20–34.

Hogenkamp DJ, Tran MB, Yoshimura RF, Johnstone TB, Kanner R, and Gee KW (2014) Pharmacological profile of a 17β-heteroaryl-substituted neuroactive steroid. *Psychopharmacology (Berl)* **231**:3517–3524.

Hosie AM, Wilkins ME, and Smart TG (2007) Neurosteroid binding sites on $GABA_A$ receptors. *Pharmacol Ther* **116**:7–19.

Joesch C, Guevarra E, Parel SP, Bergner A, Zbinden P, Konrad D, and Albrecht H (2008) Use of FLIPR membrane potential dyes for validation of high-throughput screening with the FLIPR and microARCS technologies: identification of ion channel modulators acting on the $GABA_A$ receptor. *J Biomol Screen* **13**:218–228.

Kokate TG, Svensson BE, and Rogawski MA (1994) Anticonvulsant activity of neurosteroids: correlation with γ-aminobutyric acid-evoked chloride current potentiation. *J Pharmacol Exp Ther* **270**:1223–1229.

Löscher W and Rogawski MA (2012) How theories evolved concerning the mechanism of action of barbiturates. *Epilepsia* **53 (Suppl 8)**:12–25.

Maksay G, Thompson SA, and Wafford KA (2000) Allosteric modulators affect the efficacy of partial agonists for recombinant $GABA_A$ receptors. *Br J Pharmacol* **129**: 1794–1800.

McCartney MR, Deeb TZ, Henderson TN, and Hales TG (2007) Tonically active $GABA_A$ receptors in hippocampal pyramidal neurons exhibit constitutive GABA-independent gating. *Mol Pharmacol* **71**:539–548.

Mennerick S, Chisari M, Shu HJ, Taylor A, Vasek M, Eisenman LN, and Zorumski CF (2010) Diverse voltage-sensitive dyes modulate $GABA_A$ receptor function. *J Neurosci* **30**:2871–2879.

Miller PS and Aricescu AR (2014) Crystal structure of a human $GABA_A$ receptor. *Nature* **512**:270–275.

Mortensen M, Patel B, and Smart TG (2012) GABA potency at $GABA_A$ receptors found in synaptic and extrasynaptic zones. *Front Cell Neurosci* **6**:1.

Olsen RW (2006) Picrotoxin-like channel blockers of $GABA_A$ receptors. *Proc Natl Acad Sci USA* **103**:6081–6082.

Reddy DS and Rogawski MA (2012) Neurosteroids—endogenous regulators of seizure susceptibility and role in the treatment of epilepsy, in *Jasper's Basic Mechanisms of the Epilepsies*, 4th ed (Noebels JL, Avoli M, Rogawski MA, Olsen RW, and Delgado-Escueta AV eds), National Center for Biotechnology Information, Bethesda, MD.

Rho JM, Donevan SD, and Rogawski MA (1996) Direct activation of $GABA_A$ receptors by barbiturates in cultured rat hippocampal neurons. *J Physiol* **497**:509–522.

Rissman RA and Mobley WC (2011) Implications for treatment: $GABA_A$ receptors in aging, Down syndrome and Alzheimer's disease. *J Neurochem* **117**:613–622.

Rudolph U and Möhler H (2014) $GABA_A$ receptor subtypes: Therapeutic potential in Down syndrome, affective disorders, schizophrenia, and autism. *Annu Rev Pharmacol Toxicol* **54**:483–507.

Stafstrom CE, Hagerman P, and Pessah IN (2012) Pathophysiology of epilepsy in autism spectrum disorders, in *Jasper's Basic Mechanisms of the Epilepsies*, 4th ed (Noebels JL, Avoli M, Rogawski MA, Olsen RW, and Delgado-Escueta AV eds), National Center for Biotechnology Information (US), Bethesda, MD.

Steinbach JH and Akk G (2001) Modulation of $GABA_A$ receptor channel gating by pentobarbital. *J Physiol* **537**:715–733.

Verkman AS and Galietta LJ (2009) Chloride channels as drug targets. *Nat Rev Drug Discov* **8**:153–171.

Wang M (2011) Neurosteroids and GABA-A Receptor Function. *Front Endocrinol (Lausanne)* **2**:44.

Wooltorton JR, Moss SJ, and Smart TG (1997) Pharmacological and physiological characterization of murine homomeric $\beta3$ $GABA_A$ receptors. *Eur J Neurosci* **9**: 2225–2235.

Zhao C, Hwang SH, Buchholz BA, Carpenter TS, Lightstone FC, Yang J, Hammock BD, and Casida JE (2014) $GABA_A$ receptor target of tetramethylenedisulfotetramine. *Proc Natl Acad Sci USA* **111**:8607–8612.

Address correspondence to: Isaac N. Pessah, Department of Molecular Biosciences, School of Veterinary Medicine, University of California, Davis, One Shields Avenue, Davis, CA 95616. E-mail: inpessah@ucdavis.edu

Supplemental Data for Molecular Pharmacology article:

Title: Rapid Throughput Analysis of $GABA_A$ Receptor Subtype Modulators and Blockers Using $DiSBAC_1(3)$ Membrane Potential Red Dye

Authors: Atefeh Mousavi Nik, Brandon Pressly, Vikrant Singh, Shane Antrobus, Susan Hulsizer, Michael Rogawski, Heike Wulff and Isaac N. Pessah

This file contains:

1 Supplemental figure showing two-fold diluted FMP-Red-Dye significantly changes the EC50 value for GABA on α1β3γ2 GABAAR (expressed in HEK 293 cells).

1 Supplemental figure displaying general structure of FMP-Red Dye.

1 Supplemental figure presenting FMP-red dye has the ability to detect neurosteroid PAM activity at low concentrations

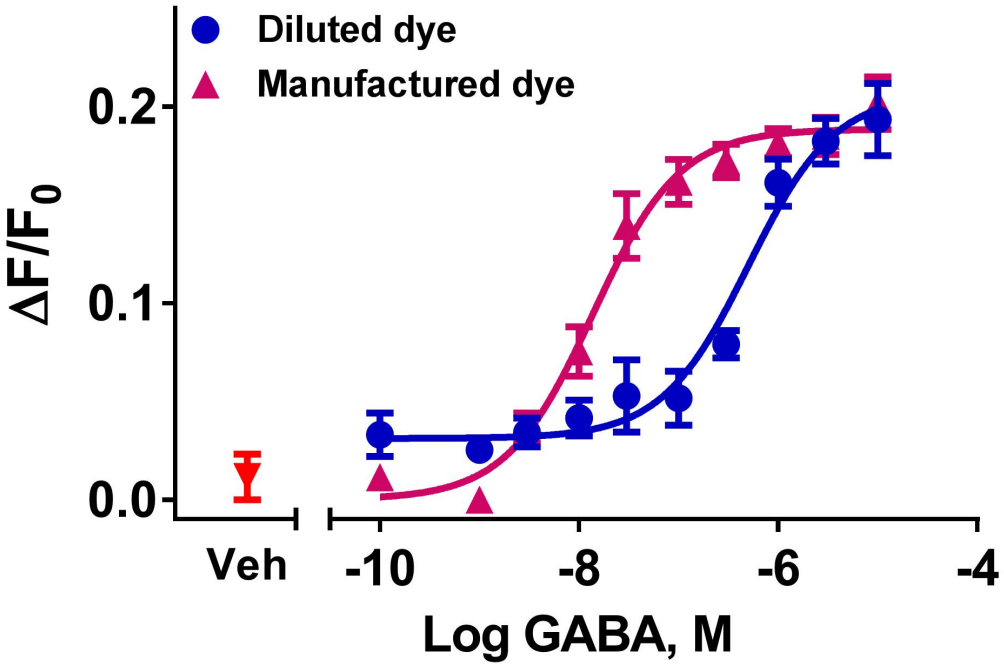

Supplemental figure 1:

Diluting FMP-Red-Dye two-fold significantly changes the EC_{50} value for GABA on α1β3γ2 $GABA_AR$ (expressed in HEK 293 cells). Using diluted dye in α1β3γ2 $GABA_AR$ (expressed in HEK 293 cells) significantly changes the GABA concentration-response curve and shifts it to the right. While the dye concentration recommended by the manufacturer provides an EC_{50} of 40 ± 11 nM, two-fold diluted dye generates an EC_{50} of 0.46 ± 0.2 μM, almost 10 times less potent. Each point represents mean ± S.E.M of data from 8 cells.

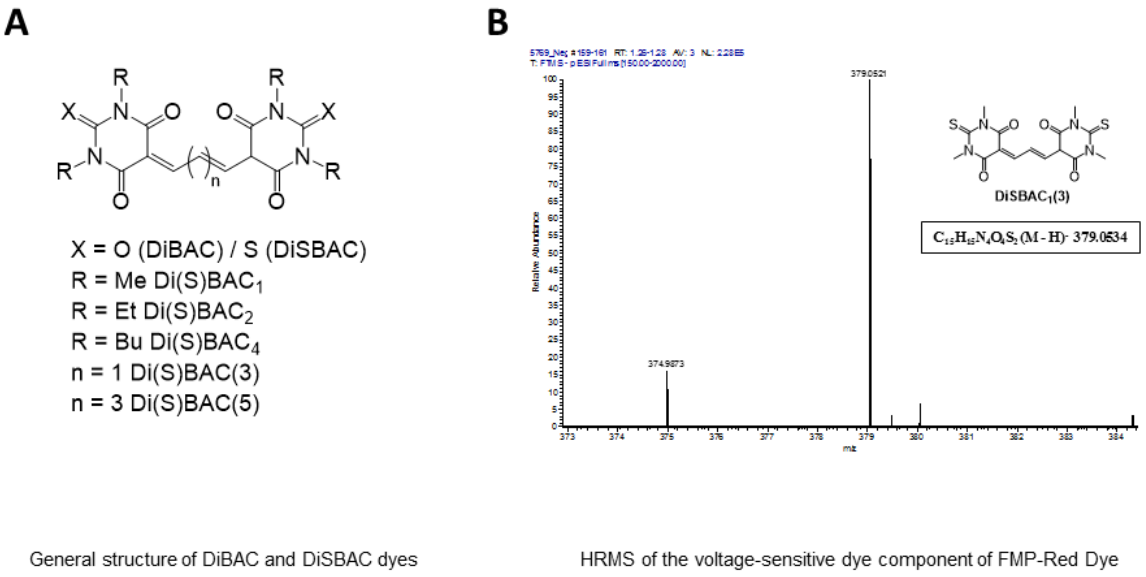

General structure of DiBAC and DiSBAC dyes

HRMS of the voltage-sensitive dye component of FMP-Red Dye

Supplemental figure 2:
General structure of FMP-Red Dye. **(A)** General structure of DiBAC and DiSBAC dyes. **(B)** High-resolution mass spectrometry (HRMS) of the voltage-sensitive dye component of FMP-Red Dye. High Resolution Mass Spectrometry (HRMS) analysis was performed by flow-injection analysis employing a Thermo Fisher Scientific LTQ Orbitrap XL Mass Spectrometer (San Jose, CA) operated in profile mode. Prior to the analysis, samples were dissolved in a mixture of 1:1 methanol and water with 0.1% formic acid added to it. Samples were injected at a flow rate of 200 µl/min. Source parameters were as following: spray voltage 5kV, capillary temperature 275 oC and sheath gas setting 20. Spectral data were acquired at a resolution setting of 100,000 full width at half maximum (FWHM) with the lockmass feature which typically results in a mass accuracy < 2 ppm. In the negative ion mode, a peak was found at m/z of 379.0521 which very strongly indicated the presence of Bis-(1,3-dimethylthiobarbituric acid) trimethine oxonol (DiSBAC1(3)). HRMS (ESI): m/z calcd. For C15H15N4O4S2 (M-H)- : 379.0534, found: 379.0521

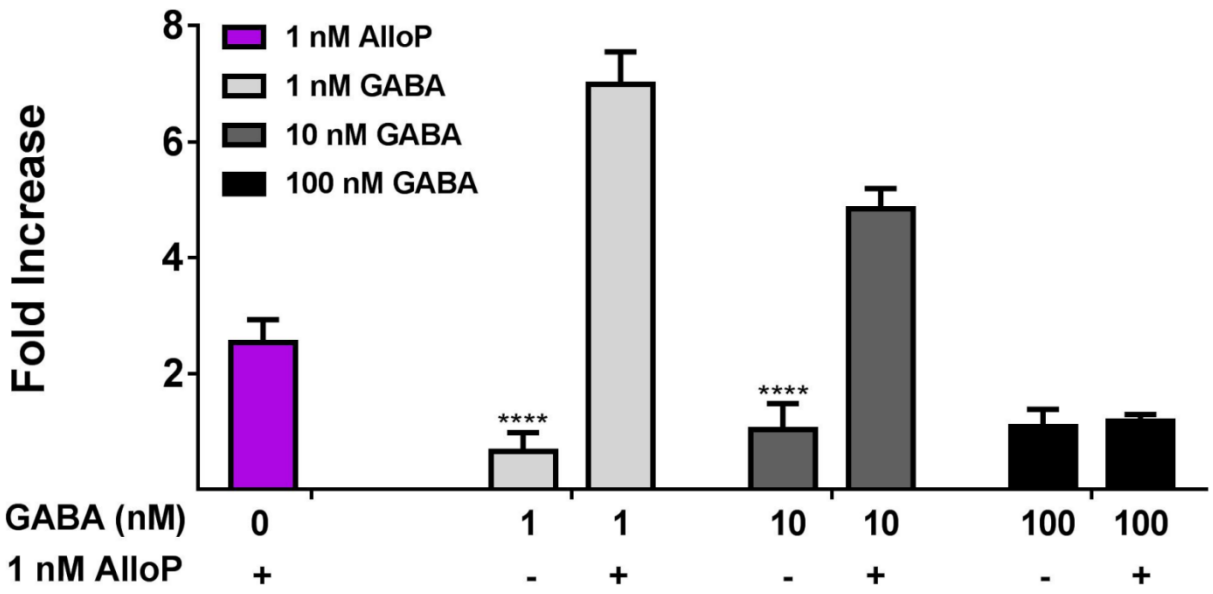

Supplemental figure 3:

FMP-red dye has the ability to detect neurosteroid PAM activity at low concentrations. In α1β3γ2 $GABA_AR$ (expressed in HEK 293 cells) 1 nM AlloP increase the AFU ~2.5 fold compared to 1 nM GABA. The neurosteroids PAM activity results in 7 and 5.5 fold increases in AFU when 1 nM AlloP is co-applied with 1 and 10 nM GABA, respectively. Applying 100 nM GABA saturates the response, therefore no difference is seen between 100 nM GABA and 100 nM GABA + 1nM AlloP. This saturation is the biggest limitation of this assay. Data were assembled from n=8. * P value <0.0001